Tectonophysics 745 (2018) 229–244

Contents lists available at ScienceDirect

Tectonophysics

journal homepage: www.elsevier.com/locate/tecto

Variability in uplift, exhumation and crustal deformation along the Transantarctic Mountains front in southern Victoria Land, Antarctica

Valerio Olivetti[a,b,*], Federico Rossetti[b], Maria Laura Balestrieri[c], Donato Pace[d], Gianluca Cornamusini[d], Franco Talarico[d]

[a] University of Padova, Dip. of Geosciences, via Gradenigo 6, 35131 Padova, Italy
[b] University of Roma Tre, Dip. of Science, Lgo S. L. Murialdo 1, 00176 Rome, Italy
[c] CNR, Istituto di Geoscienze e Georisorse, U.O.S. Firenze, via La Pira 4, 50121 Florence, Italy
[d] University of Siena, Dip. Scienze Fisiche, della Terra e dell'Ambiente, strada Laterina 8, Siena, Italy

ARTICLE INFO

Keywords:
Fission track thermochronology
Transantarctic Mountains
Rift margin
Antarctica tectonics
Antarctic topography

ABSTRACT

The Transantarctic Mountains (TAM) are an imposing topographic feature, forming the western shoulder of the Meso-Cenozoic West Antarctic Rift System. Although the TAM topography is similar to other continental rifts, some aspects such as the high topography and the transition in the mode of crustal extension from orthogonal to oblique rifting during the Cenozoic makes the TAM an anomalous rift margin. Here, we present a topography analysis of a 600 km long transect along the TAM front in southern Victoria Land combined with a large available thermochronological data-set to decode the tectonic signals hidden in the topography. An along-strike variability in tectonic, erosional and geomorphic characteristics is detected. We then focus our analysis on the Royal Society Range, where structural investigations were integrated with new fission track thermochronology in order to assess the morphotectonic evolution of the region. Fission-track data and topography of the Royal Society Range reveal remarkable differences with respect to the neighboring areas. Topography characteristics and thermal modeling suggest an increase in tectonic activity during late Eocene-early Oligocene times and structural analysis suggests that the Cenozoic rifting has been controlled by dextral transtension, as proposed for others sector of the TAM front. The detected along-strike variability in tectonic, erosional and geomorphic characteristics may reflect geodynamic complexities that should be taken into account in any further model of the TAM evolution.

1. Introduction

The Transantarctic Mountains (TAM) form the western boundary of the West Antarctic Rift System (WARS; Fig. 1), one of the largest continental rift domains on Earth, starting in the Mesozoic and still active today (e.g., Cooper et al., 1991; Salvini et al., 1997; Wörner, 1999; Fitzgerald, 2002; Rossetti et al., 2006; Storti et al., 2007; Vignaroli et al., 2015). In this regard, the TAM topography is commonly regarded as the prominent expression of a rift shoulder uplift (e.g. Gallagher and Brown, 1997; van der Beek et al., 1994; Wannamaker et al., 2017).

Morphotectonic evolution of the TAM has been commonly interpreted as genetically linked to the WARS formation. Numerous models have been proposed, spanning from flexural uplift with or without thermal contribution (Fitzgerald et al., 1986; Stern and Ten Brink, 1989; Wannamaker et al., 2017; Brenn et al., 2017) to lithosphere necking (van der Beek et al., 1994; Busetti et al., 1999). More recent studies, based on the evaluation of a thicker crustal structure across the TAM, propose they are the remnant of a Mesozoic high elevation plateau (Steinberger et al., 2004; Karner et al., 2005; Bialas et al., 2007). An alternative view has been proposed for northern Victoria Land (Fig. 1), where a scenario of dynamically supported topography by mantle flow at the edge of the Antarctic craton has been invoked to explain the Cenozoic morphotectonic evolution (Faccenna et al., 2008).

One of the main open questions regards the non-synchronicity between exhumation and tectonic phases. In the Ross Sea area (namely Victoria Land (VL) and the Ross Sea Embayment; Fig. 1), the onset of the main phase of exhumation has been postulated at about 50 Ma by the qualitative interpretation of several apatite fission-track (AFT) age – elevation vertical profiles (see Fitzgerald, 2002), and it does not correspond to the main phase of tectonic activity that seems instead to occur during late Eocene times (at ca. 35 Ma). Evidence of this tectonic activity is attested by renewed subsidence and rifting along the western

* Corresponding author at: University of Padova, Dip. of Geosciences, via Gradenigo 6, 35131 Padova, Italy.
E-mail address: valerio.olivetti@unipd.it (V. Olivetti).

https://doi.org/10.1016/j.tecto.2018.08.017
Received 25 January 2018; Received in revised form 21 August 2018; Accepted 25 August 2018
Available online 28 August 2018
0040-1951/

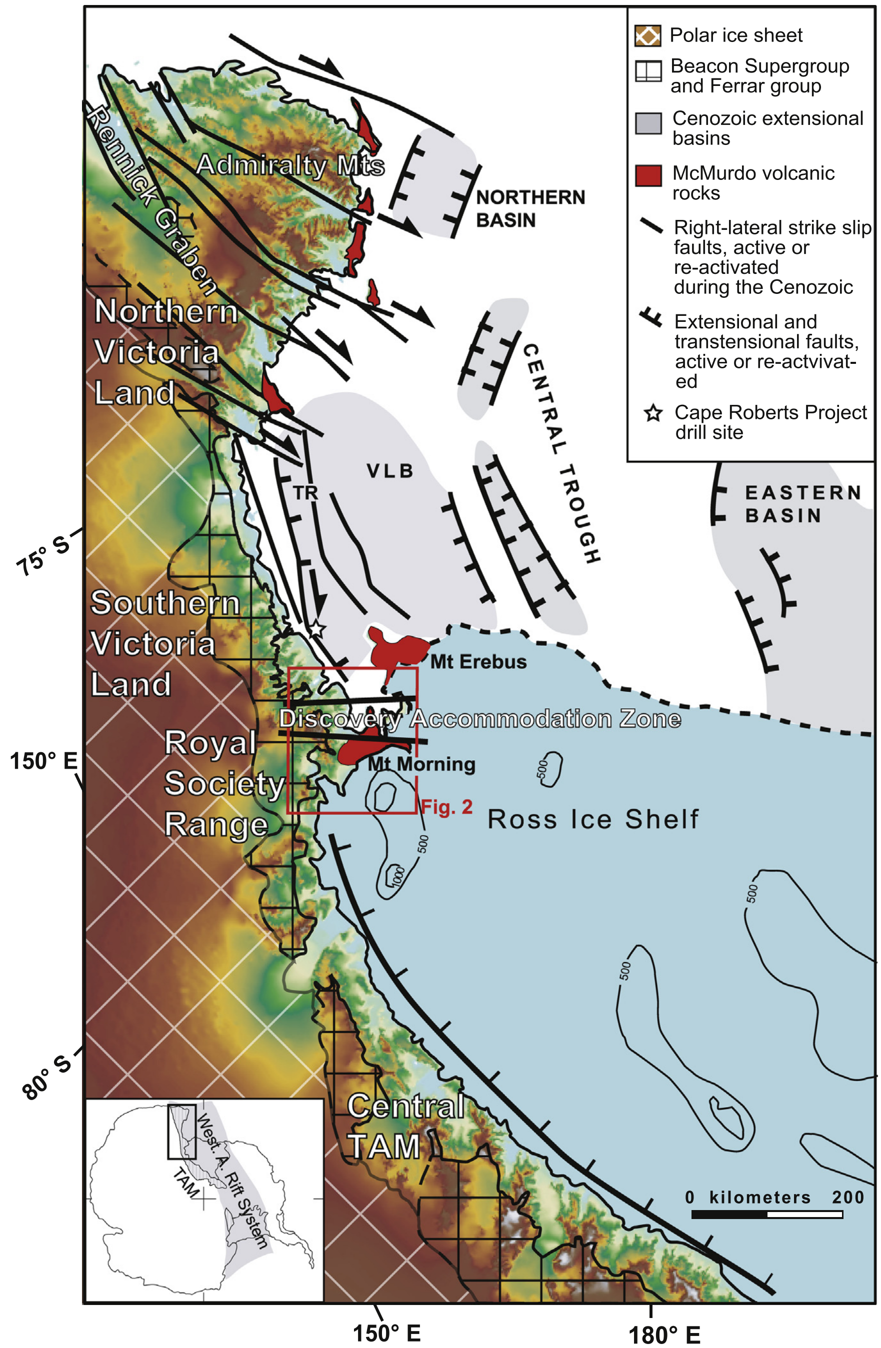

Fig. 1. Topographic relief map of the Ross Sea area and Transantarctic Mountains (TAM) showing the main topographic and bathymetric features and principal Cenozoic tectonic structures.
Modified from Salvini et al. (1997); Fitzgerald (2002); Storti et al. (2008).

Ross Sea (e.g. Terror Rift; Cooper et al., 1991; Hamilton et al., 2001), renewed fault activity (Salvini and Storti, 1999; Rossetti et al., 2003, 2006; Storti et al., 2007; Di Vincenzo et al., 2013; Vignaroli et al., 2015), and volcanic activity (Kyle and Muncy, 1989; Martin et al., 2010; Rocchi et al., 2002, 2003). This Eocene tectonic activity was coeval with and likely induced by a reorganization of the global plate tectonics circuit, occurring between 43 and 26 Ma based on Adare Trough magnetic anomalies study (Cande et al., 2000; Granot et al., 2013). Noteworthy, this tectonic reorganization is also coeval with the major climate fluctuations that have occurred at the Eocene-Oligocene boundary, during the general descent into icehouse conditions (Zachos et al., 2001).

Recently, Prenzel et al. (2013, 2018) proposed that the break in slope of an apatite fission-track (AFT) age-elevation regression provides only a minimum qualitative time constraint for the onset of exhumation that can be shifted depending on the complexity of the early thermal history. Thus, the lack of synchronicity between the onset of exhumation inferred by vertical profiles (~50 Ma) and the climax of tectonic activity (~35 Ma) could be an artifact due to long burial of the samples beneath a Mesozoic Victoria Basin (Lisker and Läufer, 2013). The sedimentary overburden would have been eroded due to basin inversion in late Eocene-early Oligocene times in response to the change in the tectonic regime from slow long-term extension to oblique rifting of the West Antarctic Rift System (Prenzel et al., 2018).

Analysis of the large-scale topography of the mountain ranges is routinely used to investigate the tectonic imprint in the Earth surface, and it is crucial to trace crustal deformation (e.g. Clark and Royden, 2000), the contribution of mantle flow (e.g. Faccenna et al., 2011) and the climate-tectonics feedback (e.g. Montgomery et al., 2001). In Antarctica this approach is limited to few studies (Stern et al., 2005; Demyanick and Wilson, 2007), because the ice hides the bedrock surface and its weight may deflect the topography by isostasy and mask the tectonic signal. On the other hand, the dry climatic conditions results in extremely low erosion rates since at least the Miocene, that are favorable to preserve stratigraphic markers of vertical crustal movements.

This study combines a topography analysis of a 600 km long transect along the TAM front with regional patterns of existing thermochronological data, providing a first attempt to recognize long wavelength tectonic signals in the present topography of Antarctica. Such data are integrated with new AFT thermochronological and structural data from the Royal Society Range (Fig. 1). The Royal Society Range shows some peculiar topographic characteristics that differ to those of the neighboring TAM regions, making it a key site to study the along-strike variations of the rift evolution: (i) the elevation is particularly high, with summits among the highest in the TAM (e.g. Mt. Lister, 4024 m), in contrast with the quite depressed area of the Dry Valleys to the north; (ii) the coast line changes orientation showing a major offset along the N-S trend of the TAM coast. The loss of the N-S linearity has been interpreted as due to a nearly E-W transverse fault system named the “Discovery Accommodation Zone” by Wilson et al. (1993) and described from satellite image and field data by Wilson (1999); and (iii) Cenozoic volcanic activity has been particularly intense forming large volcanic edifices (Mt. Morning and Mt. Discovery) that are marked by a long lasting effusive activity started at least by 18 Ma (Kyle and Muncy, 1989; Martin et al., 2010).

This work is based on a multi methodological approach that are presented in different sections: topography analysis integrated with stratigraphic marker aims to investigate the surface uplift; thermochronology is used to quantify the rock uplift and exhumation history, whereas the structural analysis aims to define the tectonic regime. We employ the synthesis of new with published data to address the following geological issues: (i) is the along-strike difference in morphology, elevation and AFT ages along the TAM margin linked to the location and differential retreat of the main escarpment (see Sugden and Denton, 2004) or to differential tectonic vertical movements (see Van der Wateren et al., 1999; Behrendt and Cooper, 1991)?; (ii) how does the tectonic regime vary along the TAM margin?

The combined results show that the Royal Society Range experienced a greater amount of rock uplift and exhumation with respect to the surrounding regions during the late Eocene-early Oligocene times, in connection with the major episode of transtensional tectonics distributed along the TAM front.

2. Geological background

The bedrock of the TAM in the Ross Sea area is chiefly made of basement units representing the exhumed roots of the late Neoproterozoic to early Paleozoic Ross Orogen, and by the early Paleozoic syn- to post-tectonic Granite Harbour Intrusives Suite (580–560 to 450 Ma, Stump, 1992; Goodge et al., 2012). The basement units are unconformably overlain by the Devonian to Lower Jurassic Beacon Supergroup (Barrett, 1991), that was deposited over a paleo-erosive surface, named Kukri Peneplain (other erosive surfaces occur within the Beacon Supergroup). The Beacon Supergroup consists mainly of fluvial sandstones with subordinate lacustrine, glacial and shallow marine sedimentary rocks (Barrett, 1991). Along the TAM, the base of the Beacon Supergroup is diachronous, being older in southern VL and Central TAM (Devonian) and younger in northern Victoria Land (Permian to Triassic), with variable thickness between 1 and ~2.5 km in central and southern VL and much less in northern VL (see Elliot and Fleming, 2004 and references therein). Despite of some regional variability, in our study area the base of the Beacon Supergroup is considered almost synchronous of Permian age (Cox et al., 2012). There, the deposits of the Beacon Supergroup attain about 2 km of thickness, showing undeformed sub horizontal bedding gently dipping westwards.

In the Middle Jurassic, at ~177 Ma (Fleming et al., 1997), the breakup of Gondwana was accompanied by considerable igneous activity that produced voluminous intrusions of Ferrar Dolerites and the extrusive Kirkpatrik Basalts with associated volcanoclastic rocks (Elliot, 1992). The thickness of the Ferrar Dolerites is variable along the TAM. In the study area, the arrangement of dolerite intrusions follow what was reported for the Dry Valleys region, where it is characterized by a sill inside the basement (up to 400 m of thickness), a sill (~100 m thick) lying on the Kukri Peneplain and several scattered minor sills within the Beacon Sandstones (Elliot and Fleming, 2004).

Occurrence of Cenozoic rocks along the TAM is limited. They consist of (i) the Sirius Group, an enigmatic thin sedimentary formation scattered along the TAM but uncertain in age (Harwood and Webb, 1998), (ii) the Eocene McMurdo erratic sandstone (Levy and Harwood, 2000) and (iii) the widely distributed magmatic products of the McMurdo Volcanic Group, spanning in age from the Eocene to Present, that form large volcanic edifices such as Mt. Discovery, Mt. Morning and Mt. Erebus (LeMasurier and Thomson, 1990).

2.1. Uplift and exhumation history of the TAM

The TAM is a ca 3500 km long mountain chain, 100 to 200 km in width, with numerous summits higher than 4000 m. Except for the northern tip of the TAM (especially the Admiralty Mountains; Fig. 1) the topographic setting shares common characteristics along the whole chain: the summits are often flat with the top surface slightly dipping toward the west, while the eastern margin is often abrupt forming locally up to 2000 m vertical walls. In general, the topography is similar to other passive and rift margins (i.e. Summerfield, 1991), with a high standing plateau (or its remnants) bordered by a main escarpment that separates the main elevations from the coastal plain and extensional basin.

The Kukri surface and the base of the Beacon Supergroup have been classically used to detect and measure the post-Beacon deposition vertical crustal movements and tectonic deformation (Katz, 1982). On the mountain summits, the Beacon Supergroup is commonly preserved, whereas along the coast it is rarely preserved (i.e. Cape Surprise, Central TAM, Miller et al., 2010). Offshore of Granite Harbour, the Cape Roberts Project (see Fig. 1 for location) drilled the Beacon sandstones at a depth of ~900 m below the sea floor and 1.5 km below s.l. (Cape Roberts Science Team, 2000), providing a first estimate of the subsidence since 34 Ma.

Uplift history of the TAM has been mainly reconstructed through fission-track thermochronology, a technique that provides a measure of the timing and rate of cooling during rock movement toward the surface (e.g. Gleadow and Duddy, 1981; Gallagher, 1995). Hence, amounts of erosion/exhumation can be derived, while direct measurement of the rock and surface uplift cannot be given (e.g. England and Molnar, 1990). The lack of Cenozoic onshore geologic and geomorphologic constraints along the TAM makes thermochronology the best method, sometimes the only one, to explore the tectonic events responsible for the crustal vertical movements. Thermochronological ages along a vertical sampling profile, such as a glacial valley flank, allow having hints on timing and rates of the progressive removal of superficial crustal thickness. Changes from older and low to younger and higher exhumation rates indicate a renewed tectonic activity. The spatial distribution of the AFT ages as derived from transverse sampling profiles across the TAM front, such as those from the Dry Valleys (Fitzgerald and Gleadow, 1990; Fitzgerald, 1992) and central TAM (Miller et al., 2010), are typical of passive and rift margins (Van der Beek et al., 1994; Brown et al., 2002) with old ages at the rear of the TAM and getting younger toward the coast. Based on the identification of changes of the exhumation rate along age-elevation plots, three main phases of accelerated exhumation were proposed, in the Early Cretaceous (~125 Ma), Late Cretaceous (~95 Ma) and Cenozoic (~50–45 Ma) (see Fitzgerald, 2002 and references therein). The tectonic significance of the first two phases of exhumation has been little examined. The urge to find an explanation for the inconsistency between the timing of the last exhumation detected by AFT data and the main tectonic phases spurred Lisker and Läufer (2013) to postulate the existence of a Mesozoic sedimentary basin in the northern VL, a portion of a larger Mesozoic Victoria Basin extending between Australia and Antarctica. Prenzel et al. (2013, 2018) reconstructed the Mesozoic–Eocene cover sequence in northern VL. In southern VL they documented the presence of the Mesozoic sedimentary cover only in the extreme northern area, in the northern Prince Albert Mountains.

The TAM front (Barrett, 1979) corresponds to a zone some tens of km wide where brittle faulting is focused and exhumation is greater. Since the pioneering work of David and Priestley (1914), the N-S linearity of the TAM front, dissected by transverse valleys, is considered as the evidence of tectonic features. Along the TAM front, faulting is partitioned into an array of NNE to NE striking normal to oblique dextral slip faults, which are usually oblique with respect to the NNW orientation of the TAM (Fitzgerald, 1992; Wilson, 1995; Salvini et al., 1997; Rossetti et al., 2006; Storti et al., 2008). The age of the Cenozoic brittle deformation is still uncertain. Some constraints, on the basis of offshore/onshore stratigraphic evidences (Salvini et al., 1997; Rossetti et al., 2003, 2006; Faccenna et al., 2008; Storti et al., 2007; Vignaroli et al., 2015), thermochronological data (Lisker, 2002), syn-tectonic magmatism (Rocchi et al., 2002) and pseudotachylite dating (Di Vincenzo et al., 2013) are available from the northern VL, where the activity of the major NW-SE dextral faults cutting across the TAM front is documented from the Eocene-Oligocene boundary till the Quaternary (Salvini et al., 1997; Rossetti et al., 2003, 2006; Storti et al., 2007). In southern VL, the dating of faulting is limited. A phase of dip slip faulting is considered coeval with the uplift of the TAM front starting at ~50 Ma, according to the age of the break in slope (Fitzgerald, 1992), whereas the transtensional kinematics seems to be later on, around 30 Ma (Wilson, 1995; Storti et al., 2008). NNE directed transtensional tectonics controlled the opening of the Cape Roberts basin at about 32 Ma (Hamilton et al., 2001). The transtensional regime is documented being active during the Pliocene and Quaternary, as attested by volcanic vent orientation (Paulsen and Wilson, 2009), the tectonic offset of Pliocene dykes (Martin and Cooper, 2010), and morphotectonic evidences (Jones, 1997).

The role of transverse faults is still debated, and they are rarely observed and mapped because covered by the large outlet glaciers draining the East Antarctic Ice Sheet. Tectonic activity along transverse accommodation zones has been postulated by changes in regional topography, inferred differences in uplift history and apparent offsets of the Kukri Peneplain surface (Tessensohn and Wörner, 1991; Behrendt and Cooper, 1991; Stump and Fitzgerald, 1992; Mazzarini et al., 1997). The age and the kinematics of the transverse faults are still debated (Jones, 1997; Wilson, 1999), too.

2.2. The Royal Society Range

The Royal Society Range encompasses an area between the Ferrar and Skelton glaciers (Fig. 2). Basement rock lithology is mainly represented by the Skelton Group, made up of marbles, schist and medium-grade metamorphic rocks, and by intrusive rocks of the Koettlitz Group (mafic intrusives), and subordinate Granite Harbour Intrusive rocks (Cox et al., 2012). The Beacon Supergroup is represented by the Devonian Taylor Group.

Thermochronological data from the Royal Society Range are less abundant than from the Dry Valleys region. Two vertical profiles analyzed through combined AFT and apatite (U-Th)/He (AHe) methods are available along the northern and southern flank of the Ferrar Glacier, recording a slightly different exhumation history for the two flanks (Fitzgerald et al., 2006). AFT ages are between 43 and 92 Ma, consistent with the Dry Valleys data, and with an Eocene accelerated exhumation rate. Recently, new AFT data were obtained along the coast of the Royal Society Range. They show ages around 30 Ma (i.e. younger than the youngest ages from the lowest elevation of Ferrar Glacier and Dry Valleys region, northwards, and from the Britannia Range, southwards), documenting an along-strike change in the exhumation pattern, probably due to rift segmentation upon transverse faults (Zattin et al., 2014).

Detrital thermochronology data on core samples from the drill core of ANDRILL Project (Zattin et al., 2010, 2012) and Cape Roberts Project (Olivetti et al., 2013), as well as drill cores clast provenance analysis (Talarico and Sandroni, 2011; Talarico et al., 2012; Cornamusini and Talarico, 2016) provided further information on the erosive and exhumation history of this sector of the TAM. Occurrence of bedrock grains with AFT ages of 40 to 20 Ma suggests an Oligocene-Miocene exhumation of the source area recognized in the Royal Society Range (Zattin et al., 2014).

The structural architecture of the Royal Society Range has been interpreted as a nearly north-south oriented horst-graben structure, controlled by NNW-SSE normal faults systems (dotted lines in Fig. 2; Gunn and Warren, 1962; Findlay et al., 1984; Fitzgerald, 1987). These fault systems define the prominent morphological escarpment of the eastern margin of the ridge and the location of the Blue Glacier (Fig. 4c). This tectonic pattern was revised by Wilson (1999) who interpreted the tectonic setting to be mainly controlled by WNW-ESE striking tectonic lineaments (including the Discovery Accommodation Zone) considered as sinistral transfer faults accommodating a different magnitude of extensional movements between different rift-flank blocks.

3. Topography analysis

3.1. Methodology

A series of swath profiles has been extracted along-strike and orthogonal to the rift margin using two data sources: (i) the Radarsat Antarctic Mapping Project (RAMP) digital elevation model (DEM) by the NASA (Liu et al., 2001), that is a 200 m resolution model of the rock and ice surface, that combines topographic data from a variety of sources collected since the 1940s, and (ii) Bedmaps2 by the British Antarctic Survey (Fretwell et al., 2013), that is a grid of a uniform 1-km spacing of surface elevation, ice-thickness, sea-floor and subglacial bed elevation derived from a variety of topographic and geophysical sources. Although other high resolution sources are available, with the aim of large scale topographic analysis, a low resolution DEM provides an already smoothed topography more suitable than a high resolution one. DEM analysis has been performed through Quantum GIS package (available at http://qgis.osgeo.org).

Over the topographic profiles, we reported the elevation of the Kukri Erosion Surface and the top of the crystalline basement. Used with care, these surfaces can be used as a landmark along the TAM front to investigate the along-strike variation of rock uplift. The main issue arises from the occurrence of Ferrar sills that intruded mainly along the Beacon/basement contact, deforming or erasing the Kukri surface. In many cases, the Ferrar sills can be used to closely establish the position of the Kukri surface.

We extracted the elevation of Kukri surface and basement top in different ways: i) after geo-referencing the geological map (1:250000 map scale of Gunn and Warren, 1962), to the Radarsat DEM; ii) for the Convoy Range, Dry Valleys, and Royal Society Range we used the 1:250000 scale geological maps recently edited by the Institute of Geological and Nuclear Science of New Zealand (Cox et al., 2012); iii) for the southern region we used the 1:1.000.000 geological maps of Craddock et al. (1969) and the paper of Foley et al. (2013). Large

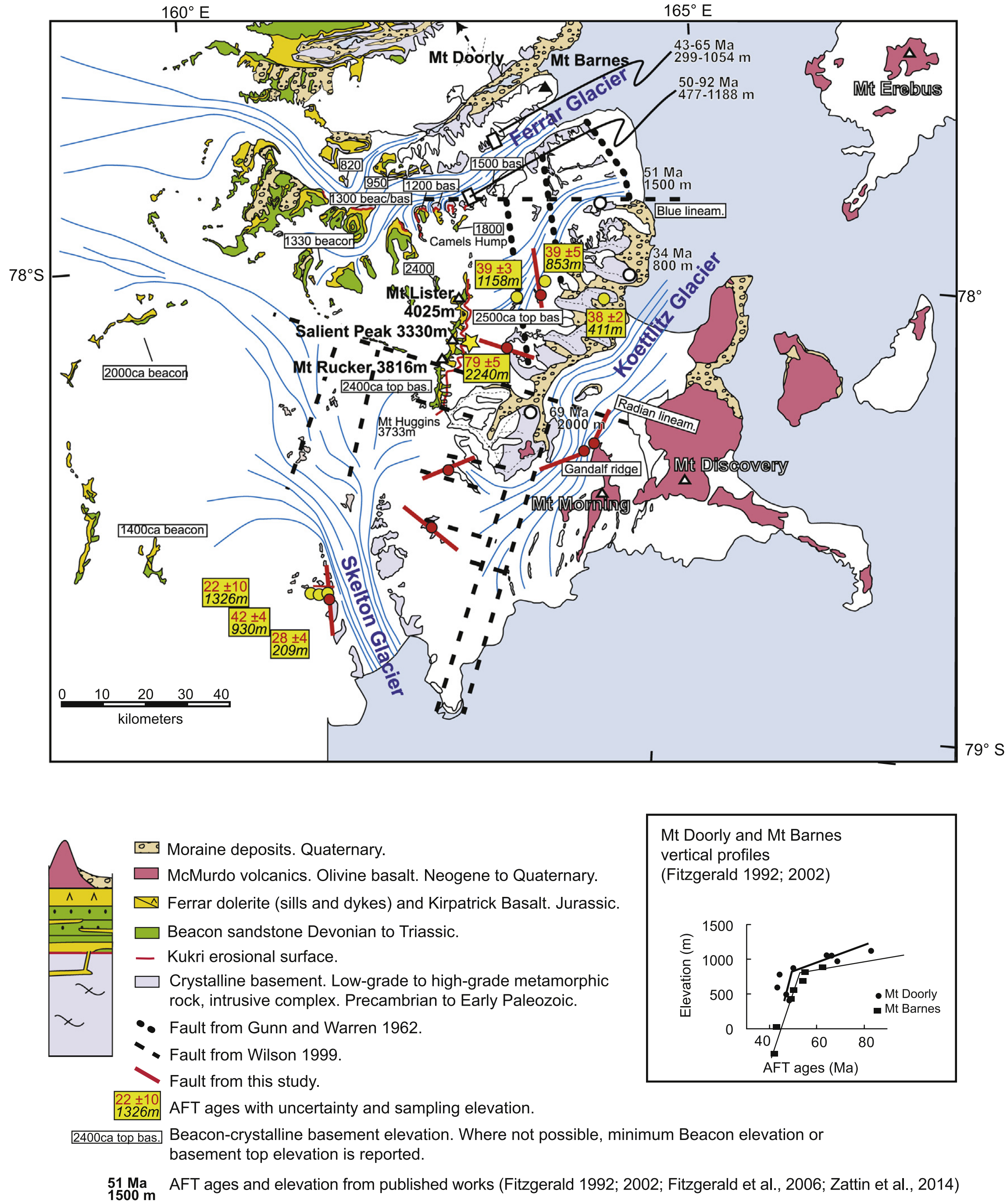

Fig. 2. Geological map of the Royal Society Range (after 1:250,000 scale geological maps of Gunn and Warren, 1962). The map shows: the contact between Beacon Supergroup and crystalline rocks (red line, Kukri Erosional Surface), the elevation of the contact, fault patterns, location of the structural analysis sites (red dots), and location of the samples for thermochronology (yellow dots) and apatite fission-track (AFT) ages. (For interpretation of the references to colour in this figure legend, the reader is referred to the web version of this article.)

uncertainties in elevation are associated to the measurements due to the variable thickness of the Ferrar Dolerites and because the Kukri surface and Basement top are often located in the middle of vertical walls where the estimate of the elevation is uncertain. Where possible, we integrated map analysis of elevation with field observation and aerial survey from helicopter.

3.2. Results: along-strike topography variation

In Fig. 3 we show four area-averaged topographic profiles (swath profiles) running parallel to the coast line covering a distance of about 600 km along the TAM. Profiles A, B and C have been extracted by the Radarsat and profile A′ from Bedmap2 sources. They cover the area of the mountain front and main escarpment. The coastal region has been ruled out to avoid that minimum curves to always assume a zero value. For this reason, the minimum topography curve is not diagnostic of the topography characteristic, reflecting often only proximity to shore line. Profiles A and A′ are reported to compare the two sources. They show very similar trends of the minimum, mean and maximum curves, with some discrepancies due to the different resolution. Larger differences occur in regions covered by large glaciers (e.g. north to Mawson Glacier).

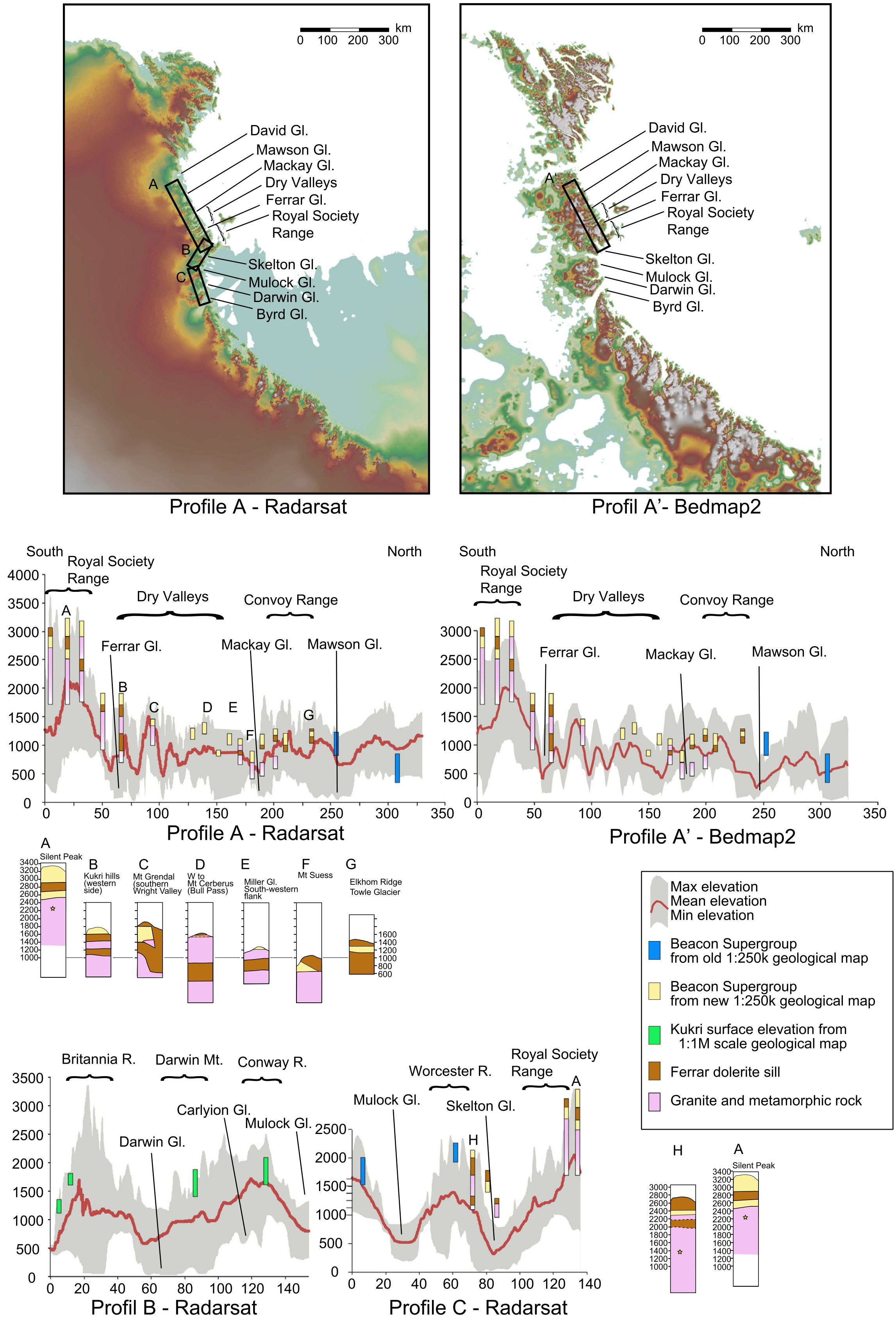

Fig. 3. Topographic maps from Radarsat and Bedmap2 data, showing swath profile traces. Radarsat is a 200 m resolution DEM, representing the rock and ice surfaces. Bedmap is a topographic and geophysical integrated model of the rock surface and ice bedrock. Swath profiles representing maximum, minimum and mean topography extracted by the Radarsat (A, B, C) and Bedmap (A') models. The boxes represent the elevation of the Beacon Supergroup, Ferrar Dolerite and Basement top to trace the Kukri erosion surface.
Sources: 1:250000 scale map: Cox et al. (2012); 1:50000 scale maps: Pocknall et al. (1994); Turnbull et al. (1994); Allibone et al. (1991). 1:250000 scale map: Gunn and Warren (1962). 1:1000000 scale map: Craddock et al. (1969).

Based on A, B and C profiles of Fig. 3, we can identify three along-strike topographic domains: (i) a northern one, from the David Glacier to the Ferrar Glacier (Convoy Range and Dry Valleys regions) characterized by mean elevation around 700 to 1000 m above sea level (asl), and maximum elevations rarely exceeding 1800–2000 m asl; (ii) the high elevated Royal Society Range, showing large areas between 3000 and 4000 m asl, (iii) a southern portion, where the topographic variations increase in amplitude due to big outlet glaciers, that separate chain regions with mean elevation around 1500 m asl and maximum elevation between 2000 and 2500 m asl.

Schematic stratigraphic sections, shown below the profiles of Fig. 3, highlight that the trend of the Kukri surface and basement top in general mimics the topography. In the northern domain the Kukri surface and basement top are found between 800 and 1400 m asl. North to Mawson Glacier (section H) and in the Convoy Range (section G) the basement top crops out around 1000 m asl, in the northern Dry Valleys (Mt. Suess, section F) at 800 m asl, whereas in the rest of the Dry Valleys region is found at approximately 1000 m asl. The maximum elevation of the Kukri surface is 1700 m asl at the Kukri Hills (section B), but it is located on top of thick dolerite sills.

In the Royal Society Range, the basement crops out at 2240 m asl (sampling site-2; Fig. 2), and no Ferrar Dolerite has been observed below this site, according to Elliot and Fleming (2004). The Peneplain Sill is traceable all along the escarpment (section A). Our field and map observation are consistent with Sugden et al. (1995) in placing the basement top between 2600 and 2200 m asl.

In the southern domain, the position of the Kukri surface and basement top is very uncertain, probably between 1500 m and 2000 m asl as derived from geological maps (Gunn and Warren, 1962). Along the Skelton Glacier, basement rocks have been sampled at elevation of 1350 m and from the helicopter view it seems to crop out till 2000 m elevation, overlain probably by Beacon Sandstone and by dolerite sill consistently with Gunn and Warren (1962) geological maps. In the Britannia Range, the Kukri surface elevation has been calculated by Foley et al. (2013) around 1700 m asl and ca. 60 km inland from the coast line.

3.3. Escarpment topography and exhumation

The along-strike variability, from north to south, in the topography of the TAM is accompanied also by a change in the mountain front morphology, as shown by the swath profiles running orthogonal to the TAM front (Fig. 4). The profiles are traced to rule out the biggest outlet glaciers. The distribution of the already published AFT ages where also presented in Fig. 4 in order to evaluate the variation along-strike of the amount of exhumation.

The swath profiles of Fig. 4 show a remarkable difference in morphology between mountain front of the Convoy Range and Dry Valleys regions, in the northern study area, and the Royal Society Range front. Convoy Range and Dry Valleys escarpment are similar and characterized by a gradual degradation of the mean and maximum elevations from the polar plateau to the coast line, along a distance of about 80 km. Higher elevations are found in the internal portion of the profiles attaining ca 2500 m. Conversely, in the Royal Society Range the topography increase from the polar plateau toward the coast, and the maximum elevation (up to 4000 m) is located at about 40 km closer to coast line with respect to the Dry Valleys. The scarp consists of an impressive wall of 2000 m. Between the main escarpment and coast line, the landscape is characterized by a low relief mainly deglaciated area with mean elevation around 1000 m (Sugden et al., 1995). The two southward profiles (Worcester Mountain and Conway Range) show a similar morphology characterized by maximum elevation around 2500 m asl located close to the coast and an abrupt main escarpment about 1000 m high.

Differences in escarpment morphology are associated to change in regional distribution of the AFT ages and exhumation. In the Dry Valleys, the old AFT ages (older than 70–80 Ma) occur either in the internal than in the coastal regions. The younger AFT ages are limited to a ca. 20 km wide band where young AFT ages (40 to 49 Ma) occurred at elevation between 500 and 800 m asl. AFT ages younger than 40 Ma are found in limited locations (e.g. New Glacier, Granite Harbour). Along the Ferrar Glacier, which separates Dry Valleys from Royal Society Range, two vertical profiles sampled for thermochronology (insert in Royal Society profile, Fig. 4c) show ages consistent with Dry Valleys ages (Fitzgerald, 1992). In the Royal Society Range, even if limited, the AFT ages younger than 40 Ma are common and mark a wide zone from the escarpment to the coast, with an elevation from 200 to 1000 m asl. South of the Royal Society Range the dominant AFT ages are younger than 40 Ma and they have been found along the coast, where they coexist with some older AFT ages (Zattin et al., 2014). Britannia Range, southernmost of the study area, represents an anomalous high topography, poorly understood, without AFT ages younger than 40 Ma (Zattin et al., 2014).

4. Thermochronology

4.1. Method

Fission tracks are linear damage zones produced in U-bearing minerals by the spontaneous nuclear fission of ^{238}U. While the production of tracks is constant, the preservation of the tracks depends on the crystalline lattice characteristics of the minerals, which in turn depend on temperature. Over geological time, fission tracks in apatites are totally retained for temperatures below 60 °C, and partially retained at temperatures between 60 °C and 120 °C (Partial Annealing zone, PAZ), (e.g. Gleadow and Duddy, 1981; Green and Duddy, 1989). The density of fission tracks represents a measure of the time over which tracks accumulate. The length of confined fission tracks is indicative of the time of residence within the PAZ (e.g. Green et al., 1986). AFT analysis consists of an age determination and measurement of a track length distribution (see Supplemental materials for details on the analytical protocols adopted in this study). A quantitative evaluation of thermal history can be obtained through the application of numerical modeling procedures. The HeFTy and QTQt software are the two most used platforms (Gallagher, 1995; Ketcham, 2005; Ketcham et al., 2000).

The interpretation of thermochronological data collected along altimetric profiles (vertical profile approach) is based on the assumption that during exhumation, a crustal section records a progressive cooling process, which leads the upper layers to emerge from the PAZ earlier than the lower ones depending on the exhumation rate. A change in the gradient in the age-elevation relationship (AER) accompanied by different length distributions upon (mean length short) and below (mean length long) indicates a transition from an old phase of slow cooling (exhumation) to a younger phase of rapid cooling (exhumation).

4.2. AFT results and modeling

The thermochronology study consists of 7 new AFT ages, two of them accompanied by a sufficient number of track length measurements (> 50) to perform thermal history modeling. Three samples were collected along a vertical profile (Skelton Glacier profile), and the others were collected along a 40 km long profile (Mt. Lister profile), that cannot be considered as vertical (Fig. 2). The sampling of the Skelton profile was carried out along the steep wall forming the western flank of Skelton Glacier and it is composed of three samples of Granite Harbour Intrusives (see the petrographic description in the Supplemental material) collected between an elevation of 200 m and 1300 m asl. The AFT ages range between 23 ± 10 Ma and 42 ± 4 Ma (Table 1).

The Mount Lister profile was carried out along an E-W directed transect between an elevation of 300 m and 2200 m asl. Some authors (Gunn and Warren, 1962; Findlay et al., 1984) inferred the presence of

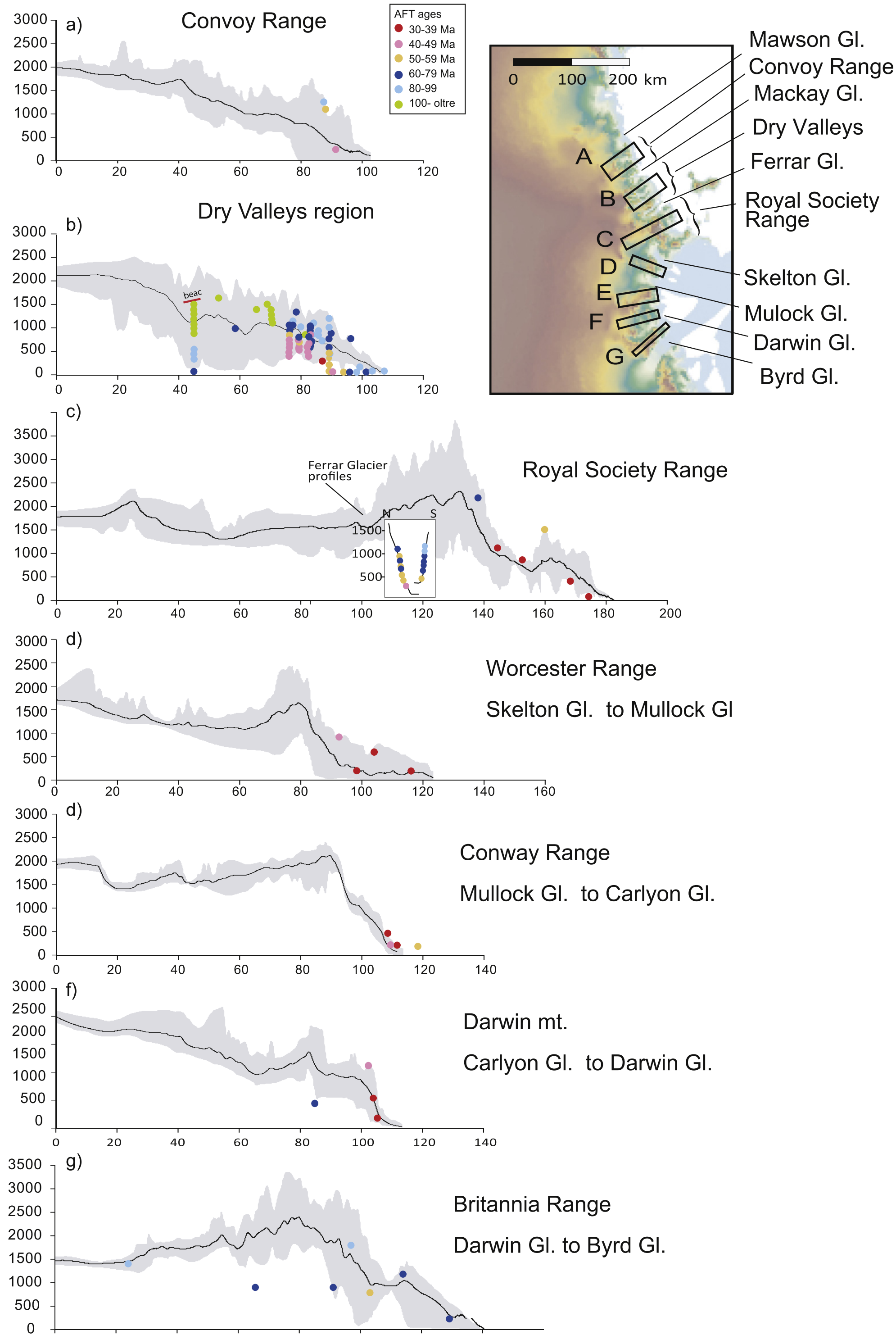

Fig. 4. Swath profiles running orthogonal to the mountain front from Radarsat source showing the topography of the main escarpment. (a) and (b) AFT ages of Convoy Range and Dry Valleys region are from Fitzgerald (1992); (c) AFT age of the Royal Society Range are from this study, Fitzgerald et al. (2006) and Zattin et al. (2014); (d, e, f, g) AFT ages are from Zattin et al. (2014).

some faults running through this profile but field campaign did not revealed them. The aim of the Mount Lister profile was to investigate the amount of exhumation in the area connecting the main escarpment rim to the coast, where already published data were available (Zattin et al., 2014). It is composed of 4 samples with AFT ages ranging between 38 ± 2 Ma and 79 ± 5 Ma. A consistent number of confined track lengths has been found and measured in the oldest (V2) and youngest samples (V9) of the Mt. Lister profile with mean track length (MTL) values of 13.3 ± 2 μm and 14.4 ± 2 μm, respectively.

Because the prior thermal history may deeply control the measured thermochronological ages, the numerical modeling is needed to quantitatively explore the onset and rate of final cooling phase. First, we performed the inverse modeling using HeFTy code (Ketcham, 2005) (Fig. 5) on the single samples V2 and V9, separately, to find the cooling histories that best fit the data.

To investigate the thermal histories, we used HeFTy in two steps: i) first we fixed four time-temperature constraints, including (1) high temperature for the Granite Harbour Intrusives emplacement (~490 Ma and ~200 °C) (2) low temperatures during Devonian to Triassic deposition of the Beacon sandstones (3) the emplacement of Ferrar dolerite (180 ± 10 Ma and 100 ± 50 °C; from our topographic analysis we know that the thickness of the overburden of our samples made of Ferrar dolerites and Beacon sandstones exceeds > 1 or 2 thousand m, still today); (4) the present day temperature (−10 °C). We allowed HeFTy to find good paths (defined as path with goodness of fitness GOF > 0.5) over 30,000 interactions, then, after HeFTy found a certain number of good paths, we refined the modeling by adding one or two extra constraints and we generated 50 good paths.

For both samples the paths that best fit the data point to a phase of accelerated cooling commencing between late Eocene and early Oligocene time (≤40 Ma). Thermal histories depicted for both samples indicate that samples reached the surface in the late Miocene at about 20 Ma, consistent with detrital AFT from marine sedimentary records (Olivetti et al., 2013). V9 sample is marked by long track lengths (14.4 ± 2 μm and 15.00 μm projected along c-axis) suggesting a rapid cooling through the PAZ. The simulated path that best fit the data show a rapid cooling between 40 Ma and 20 Ma from below the bottom of the PAZ of the order of 5–7 °C/Myr. V2 sample is marked by reduced track length (13.3 ± 2 μm and 14.12 μm projected for the c-axis) suggesting a complex thermal history. The best fit path shows a slight increase in cooling rate since 35 Ma with a rate of 3 to 1 °C/Myr, while the sample was already in the PAZ since several million years before.

To test the hypothesis of the late Eocene to early Oligocene onset for the accelerated cooling, we performed additional thermal history modeling with QTQt software (Gallagher, 2012). This modeling can be applied to a set of multiple samples of different heights from boreholes or vertical profiles, and here we tentatively applied it to the four samples from the Mt. Lister profile because field observation did not detect any faulting with relevant vertical offset along this profile. This test is used only to compare the individual sample modeling with the hypothesis that the four samples belong to the same crustal section. QTQt model for the four samples together, indicates an accelerated phase of cooling starting as late as late Oligocene to early Oligocene thus confirming the results obtained with the individual modeling with HeFTy. Concerning the possible or not occurrence of a Mesozoic Basin (Lisker and Läufer, 2013), we cannot gain information from thermal modeling due to the presence in the area of an overburden that alone can explain the temperatures of our samples before the onset of last exhumation.

5. Structural data

5.1. Method

Structural analysis has been performed with the aim to gather more information on the style and kinematics of the faults controlling rift margin deformation and regional distribution of the AFT ages in the Royal Society Range. Structural data on faults, kinematic indicators, and joints were collected at seven geo-referenced field sites, distributed from the eastern flank of Mt. Rucker to the Skelton Glacier (Figs. 2 and 3). A total of 88 faults data (fault planes and corresponding slickenlines) were collected. Recognition and characterization of the brittle structural fabrics and description of fault patterns and their kinematics was mainly based on classical criteria as derived from the analysis of the striated fault surfaces (e.g., Petit, 1987; Doblas, 1998), complemented by recognition of geological offsets in the field. The fault and fracture population analysis was performed by means of the Daisy software (http://host.uniroma3.it/progetti/fralab/).

Table 1
AFT data.

Sample	Latitude	Longitude	El. (m)	ρ_d	n_d	ρ_s	n_s	ρ_i	n_i	n_g	$P(\chi^2)$ (%)	Central age ± 1σ (Ma)	U (μg/g)	Lm ± 1σ (μm)	s.d. (μm)	n	Dpar (μm)	s.d.
V1-28	−78.690	161.380	930	8.49	3393	2.31	162	9.03	632	22	99.0	42.3 ± 4.2	11.8	–	–	–	–	–
V2-28	−78.693	161.275	1326	7.29	2887	6.0	85	21.26	301	3	< 1	22.6 ± 10.3	35.7	–	–	–	–	–
V3-28	−78.680	161.410	209	8.08	3218	2.49	195	11.84	924	26	96.0	28.3 ± 3.6	18.6	–	–	–	–	–
V2-29	−78.137	162.9085	2240	8.17	3257	10.87	1184	21.82	2377	20	77.4	78.8 ± 4.7	30.3	13.3 ± 0.2	1.8	64	2.0 (59)	0.4
V4-29	−78.049	163.4142	1158	8.26	3296	4.66	276	19.35	1145	22	83.28	38.7 ± 3.2	30.7	–	–	–	–	–
V6-29	−77.99	163.6377	853	7.34	2907	4.44	485	16.28	1776	31	98.3	38.9 ± 5.2	10.5	–	–	–	–	–
V9-29	−78.057	164.3023	411	7.98	3179	7.08	1246	28.43	5002	20	99.5	38.6 ± 2.2	41.2	14.4 ± 0.2	1.6	100	2.6 (60)	0.3

Notes: Fission-track analysis was performed in the fission-track laboratory of the CNR, Institute of Geosciences and Earth Resources.

ρ_d, ρ_i: standard and induced track densities measured on mica external detectors; ρ_s: spontaneous track densities on internal mineral surfaces, track densities are given in 10^5 tracks cm^{-2}, n_d, n_i and n_s: number of tracks on external detectors and on mineral surfaces; n_g: number of counted mineral grains; $P(\chi^2)$: (χ^2) probability (Galbraith, 1981); Central age calculated using TRACKKEY program (Dunkl, 2002); Dpar: mean etch pit diameter parallel to the c-axis and number (n) of total measured Dpar for sample; Lm: mean length of confined tracks length distribution ± standard error, s.d.: standard deviation, n: total measured lengths, only TINTs were measured, as recommended by Ketcham (2005).

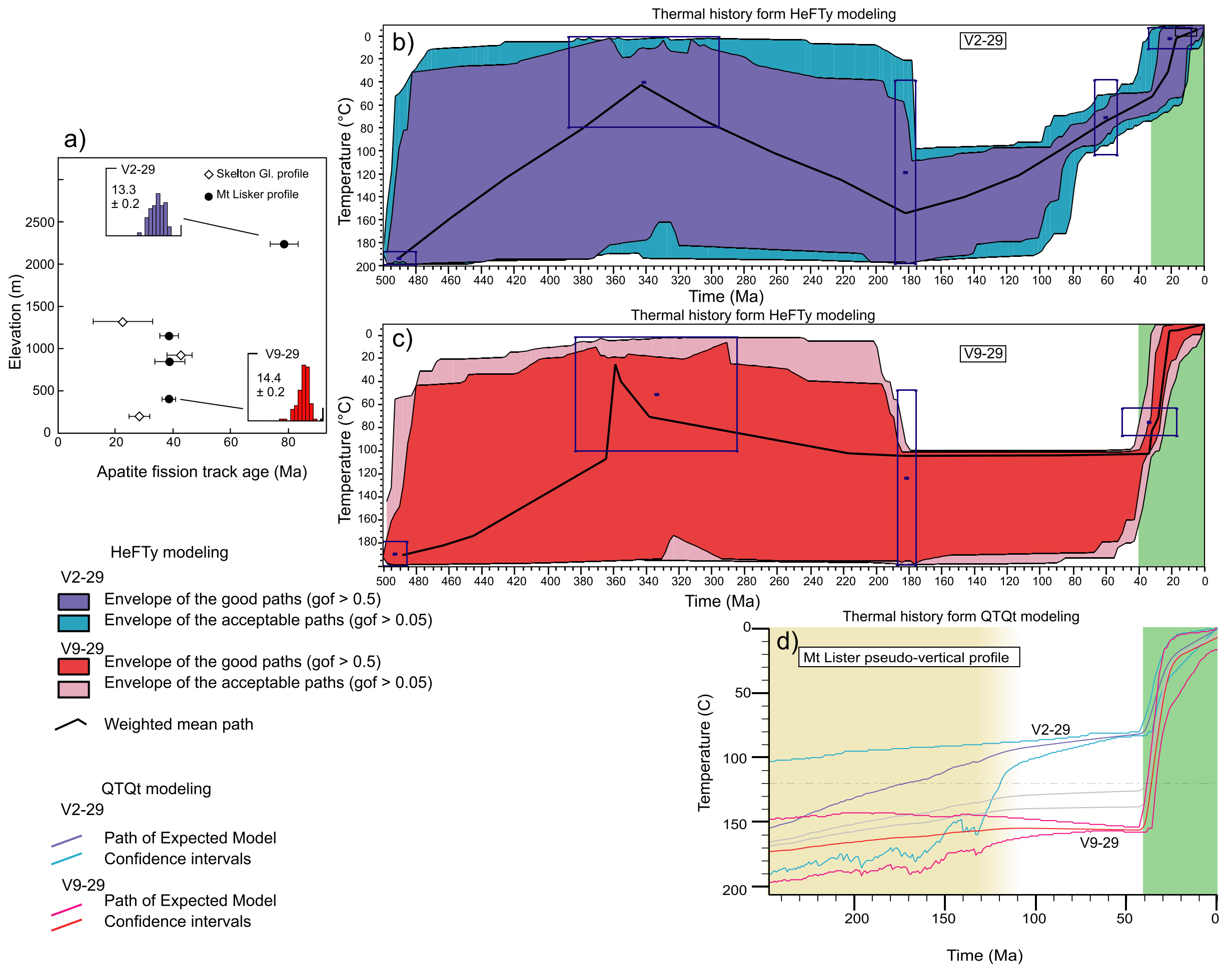

Fig. 5. (a) The graph shows new AFT ages versus sample elevation. (b, c) Thermal histories deduced from inverse modeling of AFT data of the two samples V2 and V9. Modeling was performed using HeFTy software (Ketcham, 2005). (d) Thermal history of the four samples of the Mt. Lister profile were assumed to be a vertical profile. Modeling was performed using QTQt software (Gallagher, 2012).

5.2. Results

5.2.1. Skelton Glacier

Two subsets of fault planes were measured, striking nearly N-S (330° to 20°N) and E-W (60° to 95°N), respectively (Figs. 2 and 6). The limited exposure and quality of the outcrops did not reveal any overprinting relationships between the two fault subsets. The nearly N-S striking faults are nearly parallel to the orientation of Skelton Glacier. Polished fault surfaces show kinematic indicators provided by abrasion striae, with slickenline pitch angles variable between 100° and 180°. Slickenline distribution and fault (millimeter) offsets attest to a dominant dextral kinematics. The E-W fault planes show few kinematic indicators with dispersed pitch values between 80° and 30°. Kinematic criteria, where visible, point to an overall sinistral kinematics. From aerial survey the entire wall above site-1 is characterized by N-S striking fracture arrays, parallel to the Skelton Glacier.

5.2.2. Mt. Huggins and Mt. Lister

In two sites located to the south of Mount Huggins (site-2 and -3), the exposed Granite Harbour Intrusives are affected by a set of subvertical, roughly E-W (80° to 135°N) striking, fault strands. At site-3, there is a fault zone consisting of distributed, meter-scale spaced and sub-vertical ENE-WSW oriented faults. In cross-section, curvilinear fault surfaces resemble a decameter-wide flower structure (Fig. 6a). Kinematic indicators as provided by abrasion striae and synthetic Riedel shear fractures suggest a sinistral transtensive kinematics (pitch angles of 80°, 20° and 55°N).

To the east of Mount Lister, structural data were collected along the E-W transect sampled for thermochronology (Fig. 2). Site-5 corresponds to a N-S striking fault in the geological map of Gunn and Warren (1962). There, the Granite Harbour Intrusives are affected by a major NNW-SSE striking fault zone. The fault zone is made by a decameter-wide panel of subvertical and intensely fractured rocks with numerous fault surfaces showing coexisting dip-parallel and strike-parallel slickenlines (pitch angles cluster around 90° and 170°). Kinematic indicators, as provided by abrasion striae and calcite slickenfibers, document normal and dextral kinematics, respectively (Fig. 6c). A dyke, probably Paleozoic in age, shows a dextral offset of several meters (Fig. 6b).

5.2.3. Gandalf Ridge

Structural analysis was carried out along Gandalf Ridge, at two stations previously examined by Martin and Cooper (2010). Exposed rocks consist of lithified and chaotic deposits of predominantly volcanic clasts considered to be a single sedimentary formation and interpreted as a Cenozoic diamictite lying above the basement rocks (see Martin and Cooper, 2010 and references therein). The diamictite is intruded by two generation of dykes: an E-W oriented trachyte-rhyolite dyke array with whole-rock K-Ar ages of 16–18 Ma, and a younger hawaiite dykes, dated at 3.88 Ma (whole-rock K-Ar method). The younger dyke was cut across and offset by a dextral oblique fault (Martin and Cooper, 2010).

At site-6, the diamictite and dykes are cut across and offset by a set

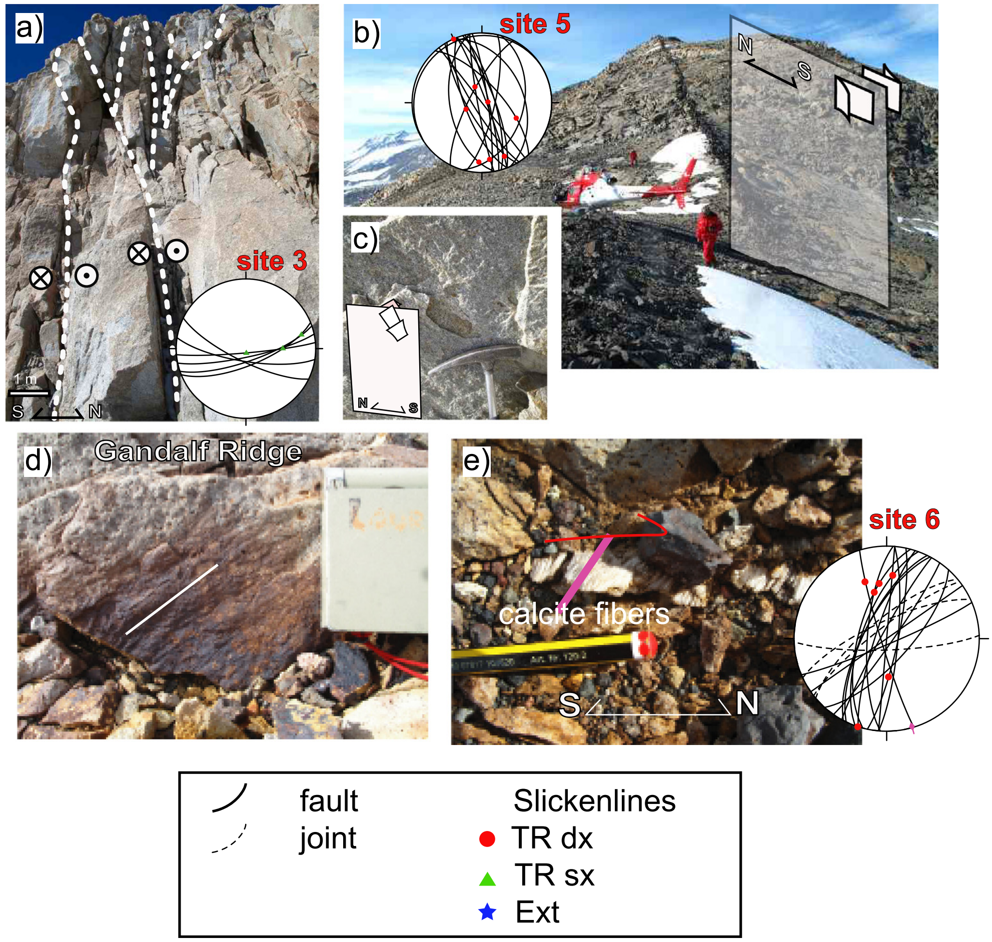

Fig. 6. Sampling sites and structural analysis sites. (a) Photograph of the site-3. Granite Harbour Intrusive is affected by faulting having half-meter-to-meter spacing; note the flower structures. (b) Photograph of site-5. Note the dextral offset dike. (c) Detail of a fault plane of site-5. Abrasion striae indicate a right normal oblique kinematics. (d) Photograph of the Gandalf ridge fault plane with hematite striae suggesting a right lateral movement. (e) Gandalf ridge site. Calcite fibers growth suggests a dextral normal oblique kinematics.

of NNE-SSW striking faults showing a decimeter wide damage zone. Polished, often hematite-coated, fault surfaces exhibit abrasion striae and calcite fibers, pointing to dextral kinematics (pitch angle of slickenlines between 160° and 180°). A transtensional component of shear is evident also by the occurrence of a subvertical NNE-SSW shear vein within a fault damage zone, with oblique growth of calcite fibers trending N130°. At site-7, a subset of nearly E-W (55° to 90°N) striking joints and faults without clear kinematic indicators are observed.

6. Discussion

The integration of the information derived from topography analysis, thermochronology and structural data support the evidence of along-strike differential vertical crustal movements along the TAM front.

In Fig. 7 we integrate the topography, the Kukri Erosion Surface and basement top elevations with the AFT age-elevation relationships (AER) to take into account the exhumation at regional scale. Moving from north to south along the profile (Fig. 7) we remark that between David and Ferrar Glaciers the trend of the topography and the elevation of the Kukri Erosion Surface and basement top show a similar trend and consistent elevation around 1500 and 1000 m. The AER diagrams for the Dry valleys region and Prince Albert Mountains show similar trend, suggesting a similar exhumation history. In both regions, the majority of the AFT ages span between 40 and 80 Ma, with only few ages younger than 40 Ma, and the AFT ages show large variations at lower elevation and along the coastal region, reflecting down-faulting of crustal blocks toward the coast (see also Fitzgerald, 1992, 2002).

In the Royal Society Range, the high elevation matches the higher elevation of the Kukri Surface and basement top, as reported by our field observations and by published data (Sugden et al., 1995). AFT ages are shifted toward higher elevation than compared to the Dry Valleys: samples having AFT ages of 40 to 50 Ma, are found 500 to 1000 m higher in the Royal Society Range respect to the Dry Valleys. The matching of higher topography with Kukri Surface and basement top higher elevations suggests that rock uplift is the main reason for the higher topography. Simple erosion cannot be responsible because in that case AFT samples of the same ages would be expected either to have the same elevation in both regions; or to be older at the top of the Royal Society Range. Thus, rock uplift along the main axis of the Royal Society Range is greater than in the Dry Valleys.

We remark that AFT ages from both flanks of the Ferrar Valley are very similar to the Dry Valleys (Fig. 7), suggesting that the change in AFT trend should occur south of the Ferrar Glacier and before the abrupt increase in topography of the Royal Society Range.

From HeFty thermal modeling, the average cooling rate derived for V9 sample between 40 and 22 Ma is ca 5 to 8 °C/Myr, corresponding to a 0.31–0.22 km/Myr rate of exhumation (for a geothermal gradient of 25 °C/km). These values can be compared, with caution, with those estimated for the Dry Valleys region. Caution must be taken because the AFT data from Dry Valleys have never been modeled and, therefore the comparison is based on data obtained through different methods and

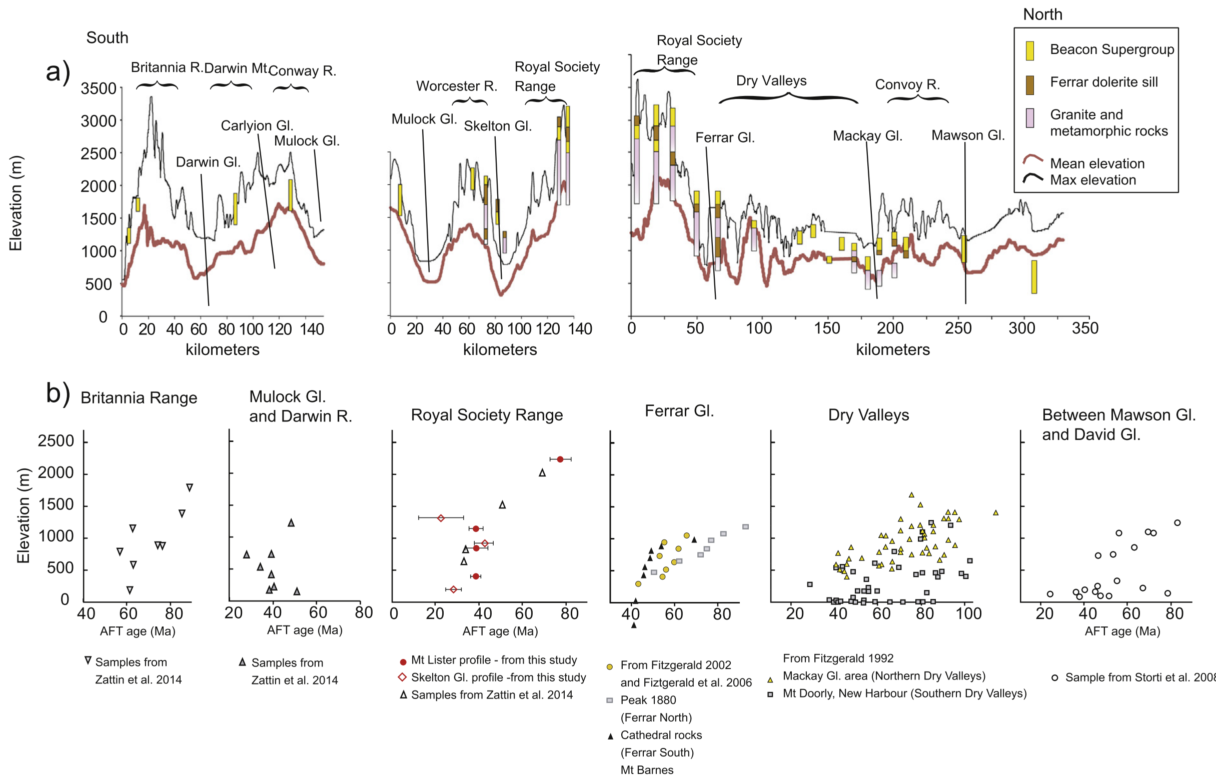

Fig. 7. (a) Swath profiles along the TAM front: red line is the mean topography, yellow bars are the elevation of the base of the Beacon Supergroup. (b) Apatite fission track ages versus samples elevation for vertical profiles carried out at different locations along the TAM front. (For interpretation of the references to colour in this figure legend, the reader is referred to the web version of this article.)

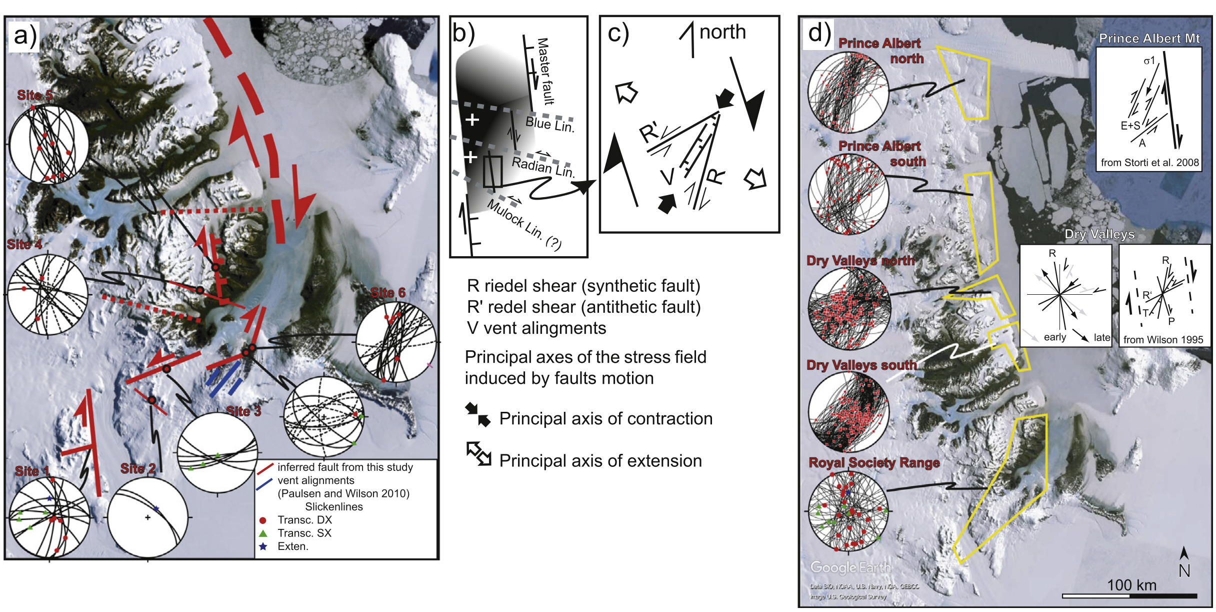

Fig. 8. (a) Satellite image with new structural data (Schmidt projection, lower hemisphere). The red lines correspond to the tectonic setting inferred by structural data. (b) Sketch showing the deformation architecture of the Royal Society deformation zone. (c) The inset shows the angular and genetic relationships between master right lateral strike-slip fault systems (thick line) and subsidiary faults in their damage zones. (d) Satellite image with structural data that summarize the structural data and interpretation of the tectonic setting along-strike the TAM. Data and interpretation of Prince Albert Mountains are from Storti et al. (2008), data and interpretation of the Dry Valleys are from Wilson, 1995; data of the Royal Society Range are from this study.

the result could be biased. Exhumation rates of the Dry Valleys can be calculated by a regression of the AER (Mt. Doorly, Mt. England, Mt. Newall and Mt. Barnes) for the time comprised between 40 and 50 Ma. The estimated exhumation rate is ca 0.1 ± 0.1 km/Myr (Fitzgerald, 1992, 2001), remarkably lower than what obtained from modeling of sample V9 of the Royal Society Range. Therefore, we interpret the AFT ages from the Royal Society as evidence of accelerated exhumation post 40 Ma. It is not possible to constrain the onset of the accelerated exhumation phase because for the Royal Society Range data are few, and cannot be extrapolated to the entire region.

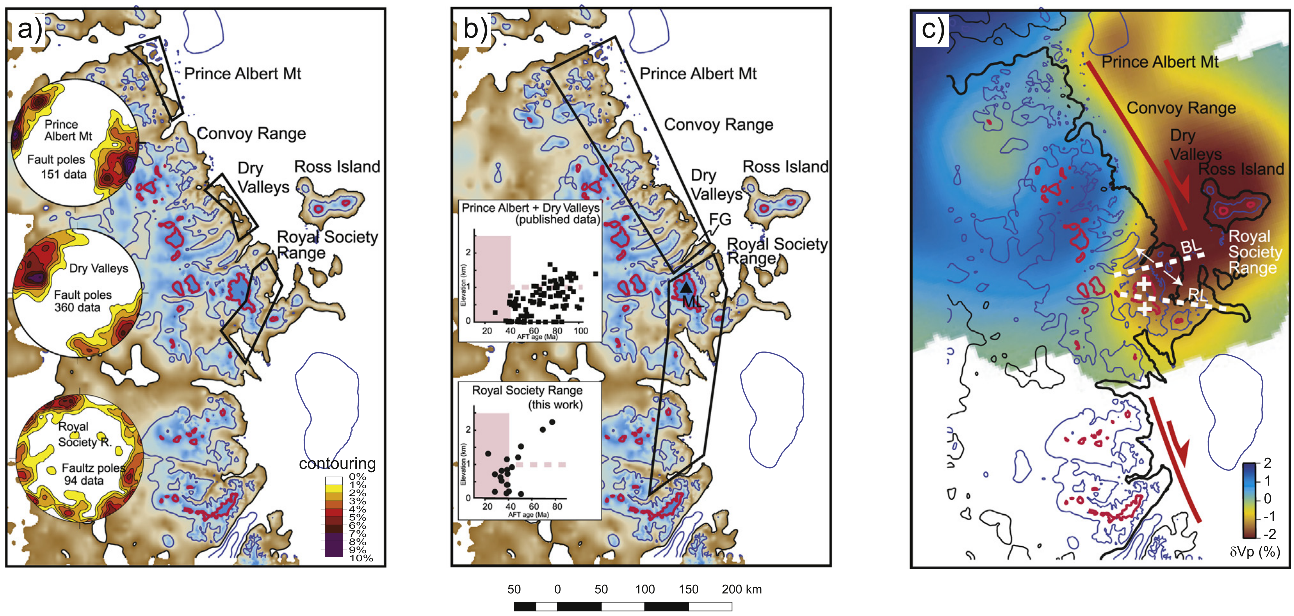

Fig. 9. (a) Topographic relief maps with cumulative fault poles distribution showing the variability between the Prince Albert Mountain-Dry Valleys and the Royal Society Range where the fault poles are scattered. (b) The figure summarizes the along-strike variability in the AFT showing that in Royal Society Range the age younger than 40 Ma are more abundant and elevated. (c) Topography and focused uplift is compared with the high temperature anomaly localized by Brenn et al. (2017). The white lines are the transverse tectonic features: BL Blue Lineament, RD Radian Lineament, ML Mount Lister, FG Ferrar Glacier.

Detrital thermochronological analysis of the Cape Roberts Project drill cores, located in front of the Dry Valleys coasts (Olivetti et al., 2013) (Fig. 1), may help to constrain the uplift history of the Royal Society Range. Detrital samples between stratigraphic age of 29 and 24 Ma show a well statistically defined AFT peak age younger than 40 Ma (36 to 32 Ma) of likely provenance from the Royal Society Range (Olivetti et al., 2013, 2015). The evolution of this age peak through time gives a lag time of 10 Myr, suggesting an exhumation rate on the order of 0.4 km/Myr, remarkably higher than the exhumation rate between 50 and 40 Ma from the Dry Valleys vertical profiles.

The numerous AFT ages younger than 40 Ma from the Royal Society Range suggest that the late Eocene/early Oligocene exhumation was widespread and involved a remarkable crustal thickness, in agreement with the sedimentary records from the proximal marine basins.

6.1. Tectonic scenario

Since new structural data are limited and age of faulting is uncertain, the structural analysis alone is not sufficient to sustain a new tectonic model for the deformation of the Royal Society Range. Nevertheless, measured data can be integrated and compared with existing structural data (Wilson, 1995, 1999; Storti et al., 2008) in order to reconsider some aspects of the previously proposed tectonic model for the evolution of this sector of the TAM.

The brittle deformation of the Royal Society Range consists of a complex array of NNE-SSW and ENE-WSW fault strands, with nearly WNW-ESE striking faults, with NE-SW joints (Fig. 8a). Dextral kinematics predominates. The study area display diffuse deformation and master faults are not observed. The majority of the measured faults are interpreted to be subsidiary shears such as synthetic (R) and antithetic (R') Riedel shears, hypothesized to be conjugate systems formed under a regional transtensional dextral shear regime in response to a NE-SW directed maximum compression and NW-SE maximum extension direction (Fig. 8b, c).

In our field work, from the Mt. Lister main escarpment and the coast, no important N-S normal faults were observed. Site 5 (Fig. 8a) corresponds to an inferred fault reported in Gunn and Warren (1962) maps presumed to be one of the main tectonic features responsible for the main scarp, range uplift and graben fault arrangement hypothesized by (Gunn and Warren, 1962). The dextral fault we identified has limited offset and the young AFT ages along the coast suggest that normal offsets are limited. The transtensional tectonic scenario we depicted in the Royal Society Range (Fig. 8c) is compatible with the occurrence in the field of NE-SW striking joints and vein arrays and with the NE-SW orientation of Mt. Morning volcanic vents (Paulsen and Wilson, 2009). In Fig. 8d, we show the structural data from Wilson (1995) and Storti et al. (2008) to illustrate the regional variability of the fault array. The NN*E*- and NE-directed faults that predominate in the Prince Albert Mountains and Dry Valleys are well represented also in the Royal Society Range. In general, fault trends in the Royal Society Range appear more scattered with numerous planes showing a N and a NW strike. Scattering is probably due to the role of orthogonal structures such as Blue Lineament and Radian Lineament (Discovery Accommodation Zone of Wilson, 1999), that could have been reactivated as transfer faults and made the deformation pattern more complex.

Taking all evidences together, we interpret the regional stress regime along the Royal Society Range as responsible for a N-S dextral transtensional scenario during the last 35 Myr, that is similar to the tectonic scenario proposed for the sector of the TAM immediately north of the Royal Society Range and in northern VL (Wilson, 1995; Storti et al., 2008) and for the opening of the Cape Roberts Basin (Hamilton et al., 2001) and Terror Rift (Salvini et al., 1997; Rossetti et al., 2003, 2006; Storti et al., 2001, 2007, 2008). Our model differs from Wilson (1999) that found in the Royal Society Range evidence for orthogonal rifting during E-W extension and Jones (1997) that emphasized dextral strike-slip faults active until the Quaternary.

6.2. Synthesis and geodynamics implications

The along-strike variability in fault patterns, topography and exhumation are summarized in Fig. 9. In general, the distribution of fault orientation (Fig. 9a) is similar along the entire TAM front, with an evident variability in the Royal Society Range where the fault directions are more dispersed. Similarly, the AFT ages are different in the Royal Society Range, where ages younger than 40 Ma are abundant and found at higher elevation (Fig. 9b). Also the topography and rock uplift is remarkably higher in the Royal Society Range.

We suggest that these observed variabilities could be produced by the thermal state of the upper mantle beneath the Royal Society Range. In fact, it is noteworthy that the boundary between the Prince Albert Mountain-Convoy Range-Dry Valleys region and the higher topography and higher exhumation region of the Royal Society Range matches exactly the limit of the low-velocity anomaly of the P- and S-waves in the upper mantle (Brenn et al., 2017) (Fig. 9c). Low velocity of the seismic waves is produced by a high-temperature anomaly localized in the upper mantle at 100–150 km of depth. The shape of the high-temperature anomaly is N-S elongated and coincident with the Terror Rift where Cenozoic extension is focused. Toward the south, the high temperature anomaly extends beneath the Royal Society Range, enhancing the rock uplift, consequent exhumation, and volcanism.

In this scenario, the dextral oblique kinematics may have played a crucial role in the origin of the temperature anomaly in the region. When the dextral transtension became dominant in the Royal Society Range, around 35 Ma, the WNW-ESE crustal structures, probably inherited from the Ross orogeny, being nearly orthogonal to the regional extension direction had a suitable orientation to be reactivated (Fig. 9c) enhancing decompression melting in the mantle and magma rising. In particular, since the abrupt change in topography and AFT ages between Mount Lister and Ferrar Glacier (Fig. 9b), the Blue Lineament (Fig. 9c; Findlay et al., 1984; Wilson, 1999) appears as the best candidate to have accommodated the uplift of the Royal Society Range. The Rock uplift and exhumation were then likely caused by the subsequent magmatic underplating at the base of the extending crust. This scenario suggests that the today observed high temperature anomaly was originated in the late Eocene-early Oligocene times.

This time corresponds to a major tectonic reorganization of the TAM front, in the proximal basins and in the entire WARS; accelerated opening of Terror Rift and onset of Cape Roberts Basin occur around 35 Ma, as well as strong fault activity (Di Vincenzo et al., 2013; Rossetti et al., 2006) and the transition from pure dip-slip to dextral/oblique kinematics (Wilson, 1995; Salvini and Storti, 1999, Salvini et al., 1997; Rossetti et al., 2003, 2006), while the Adare Trough recorded the major phase of extension (from 43 to 26 Ma; Cande et al., 2000). A discrepancy remains on the age of the onset of exhumation and uplift of the margin. Onset of exhumation is hypothesized between 45 and 55 Ma for the Dry Valleys (Fitzgerald, 1992), 10 to 20 Myr earlier than in the Royal Society Range. Two phases of tectonic activity have been also implicitly suggested by many authors for the Victoria Land (e.g. Sugden and Denton, 2004). Prenzel et al. (2013, 2018) propose only one phase of exhumation starting in late Eocene-early Oligocene and they interpreted the 50 Ma event as an artifact in the AER due to the complex earlier history of the studied samples. On the other hand, the two phases of rift shoulder uplift could correspond to a transition from a style of slow wide rifting to a faster narrow rifting of the WARS. The age of the onset of the exhumation remains one of the topical issue for the TAM evolution.

7. Concluding remarks

The overlapping of the high topography and high exhumation with a high temperature anomaly of the upper mantle recently well localized beneath of the Royal Society Range (Brenn et., 2017) suggests a thermal contribution to the crustal uplift and enhanced rock exhumation in the region. Moreover, the thermal anomaly could have been enhanced by the Cenozoic transtensional tectonics in the late Eocene-early Oligocene, concomitantly with the major tectonic reorganization all along the TAM front and proximal basins.

In the Royal Society Range, the interplay of the Cenozoic N-S tectonic structures with the orthogonal lineaments, such as Blue Lineament and Radian Lineament, forming the Discovery Accommodation Zone (Wilson, 1999), led to a tectonic arrangement that facilitated reworking and reactivation of the continental lithosphere, crustal stretching and magmatic underplating at depth. Feedbacks and interactions among these processes have been responsible for enhanced rock exhumation and topography in the region.

Acknowledgements

The authors would like to thank two anonymous reviewers and Andreas Läufer for their constructive and accurate revision that significantly contributed to improve the final version of the manuscript. The research was carried in the framework of the research projects PDR2013/AZ2.07 (coordinated by F. Rossetti) and PDR2009/A2.19 (coordinated by F. Talarico) both founded by PNRA (Italian Research Program in Antarctica). We are warmly grateful for the logistics provided by the PNRA and ENEA-UTA (expedition leader: A. Della Rovere), and acknowledge the “Helicopters New Zealand (HNZ)” pilots (Ricky Park in particular), and all colleagues sharing time in the Italian base “Mario Zucchelli”. The paper benefits from constructive discussions with Massimiliano Zattin.

Appendix A. Supplementary data

Supplementary data associated with this article can be found in the online version, at https://doi.org/10.1016/j.tecto.2018.08.017. These data include the Google map of the most important areas described in this article.

References

Allibone, A.H., Forsyth, P.J., Sewell, R.J., Turnbull, I.M., Bradshaw, M.A., 1991. Geology of the Tundergut Area, Southern Victoria Land, Antarctica. 1:50000. New Zealand Geological Survey Miscellaneous Geol. Map 21. Department of Scientific and Industrial Res, Wellington, New Zealand.

Barrett, P.J., 1979. Proposed drilling in McMurdo Sound. Mem. Natl. Inst. Polar Res. Spec. Issue 13, 231–239.

Barrett, P.J., 1991. The Devonian to Jurassic Beacon Supergroup of the Transantarctic Mountains and Correlatives in Other Parts of Antarctica: The Geology of Antarctica. Clarendon Press, Oxford, pp. 120–152.

Behrendt, J.C., Cooper, A., 1991. Evidence of rapid Cenozoic uplift of the shoulder escarpment of the Cenozoic West Antarctic rift system and a speculation on possible climate forcing. Geology 19, 315–319.

Bialas, R.W., Buck, W.R., Studinger, M., Fitzgerald, P.G., 2007. Plateau collapse model for the Transantarctic Mountains–West Antarctic Rift System: insights from numerical experiments. Geology 35 (8), 687–690.

Brenn, G.R., Hansen, S.E., Park, Y., 2017. Variable thermal loading and flexural uplift along the Transantarctic Mountains, Antarctica. Geology 45 (5), 463–466.

Brown, R.W., Summerfield, M.A., Gleadow, A.J., 2002. Denudational history along a transect across the Drakensberg Escarpment of southern Africa derived from apatite fission track thermochronology. J. Geophys. Res. Solid Earth 107 (B12).

Busetti, M., Spadini, G., Van der Wateren, F.M., Cloetingh, S., Zanolla, C., 1999. Kinematic modelling of the west Antarctic rift system, Ross Sea, Antarctica. Glob. Planet. Chang. 23 (1), 79–103.

Cande, S.C., Stock, J.M., Muller, R.D., Ishihara, T., 2000. Cenozoic motion between East and West Antarctica. Nature 404, 145–150.

Cape Roberts Science Team, 2000. Studies from Cape Roberts Project. Initial Report on CRP-3. Terra Antarct. 7, 1–209.

Clark, M.K., Royden, L.H., 2000. Topographic ooze: building the eastern margin of Tibet by lower crustal flow. Geology 28 (8), 703–706.

Cooper, A.K., Davey, F.J., Hinz, K., 1991. Crustal extension and origin of sedimentary basins beneath the Ross Sea and Ross Ice Shelf, Antarctica. In: Thomson, M.R.A., Crame, J.A., Thomson, J.W. (Eds.), Geol Evolution of Antarctica. Cambridge Univ. Press, Cambridge, pp. 285–291.

Cornamusini, G., Talarico, F.M., 2016. Miocene Antarctic ice dynamics in the Ross Embayment (Western Ross Sea, Antarctica): Insights from provenance analyses of sedimentary clasts in the AND-2A drill core. Glob. Planet. Chang. 146, 38–52.

Cox, S.C., Turnbull, I.M., Isaac, M.J., Townsend, D.B., Smith Lyttle, B., 2012. Geology of Southern Victoria Land, Antarctica: Scale 1:250,000. GNS Science. Institute of Geological & Nuclear Sciences, Lower Hutt.

Craddock, C., et al., 1969. Geologic maps of Antarctica: American Geographical Soc., folio 12, scale 1:1,000,000.

David, T.W.E., Priestley, R.E., 1914. Glaciology, physiography, stratigraphy and tectonic geology of south Victoria Land. In: Reports of Scientific Investigations - British Antarctic Expedition, pp. 1907–1909.

Demyanick, E., Wilson, T.W., 2007. Morphotectonic architecture of the Transantarctic Mountains rift flank between the Royal Society Range and the Churchill Mountains based on geomorphic analysis. In: Cooper, A.K., Raymond, C.R. (Eds.), Antarctica: A Keystone in a Changing World – Online Proceedings of the 10th ISAES. USGS Open-File Report 2007-1047, Short Res. Paper 096pp. 6. https://doi.org/10.3133/of2007-

1047.srp096.
Di Vincenzo, G., Rossetti, F., Viti, C., Balsamo, F., 2013. Constraining the timing of fault reactivation: Eocene coseismic slip along a Late Ordovician ductile shear zone (northern Victoria Land, Antarctica). GSA Bull. 125 (3/4), 609–624. https://doi.org/10.1130/B30670.1.
Doblas, M., 1998. Slickenside kinematic indicators. Tectonophysics 295 (1-2), 187–197.
Dunkl, I., 2002. Trackkey: a Windows program for calculation and graphical presentation of fission track data. Comput. Geosci. 28 (1), 3–12.
Elliot, D.H., 1992. Jurassic magmatism and tectonism associated with Gondwanaland break-up: an Antarctic perspective. Geol. Soc. Lond. Spec. Publ. 68 (1), 165–184.
Elliot, D.H., Fleming, T.H., 2004. Occurrence and dispersal of magmas in the Jurassic Ferrar large igneous province, Antarctica. Gondwana Res. 7 (1), 223–237.
England, P., Molnar, P., 1990. Surface uplift, uplift of rocks, and exhumation of rocks. Geology 18 (12), 1173–1177.
Faccenna, C., Rossetti, F., Becker, T.W., Danesi, S., Morelli, A., 2008. Recent extension driven by mantle upwelling beneath the Admiralty Mountains (East Antarctica). Tectonics 27 (4).
Faccenna, C., Molin, P., Orecchio, B., Olivetti, V., Bellier, O., Funiciello, F., Minelli, L., Piromallo, C., Billi, A., 2011. Topography of the Calabria subduction zone (southern Italy): clues for the origin of Mt. Etna. Tectonics 30 (1).
Findlay, R.H., Skinner, D.N.B., Craw, D., 1984. Lithostratigraphy and structure of the Koettlitz Group, McMurdo Sound, Antarctica. N. Z. J. Geol. Geophys. 27, 513–536.
Fitzgerald, P.G., 1987. Uplift History of the Transantarctic Mountains in the Ross Sea Sector and a Model for their Formation. Univ. of Melbourne, Victoria, Australia, pp. 327 (PhD Dissertation).
Fitzgerald, P.G., 1992. The Transantarctic Mountains of southern Victoria Land: the application of apatite fission track analysis to a rift shoulder uplift. Tectonics 11, 634–662.
Fitzgerald, P.G., 2002. Tectonics and landscape evolution of the Antarctic plate since the breakup of Gondwana, with an emphasis on the West Antarctic Rift System and the Transantarctic Mountains. R. Soc. N. Z. Bull. 35, 453–469.
Fitzgerald, P.G., Gleadow, A.J.W., 1990. New approaches in fission track geochronology as a tectonic tool: examples from the Transantarctic mountains. Nucl. Tracks 17, 351–357.
Fitzgerald, P.G., Sandiford, M., Barrett, P.J., Gleadow, A.J., 1986. Asymmetric extension associated with uplift and subsidence in the Transantarctic Mountains and Ross Embayment. Earth Planet. Sci. Lett. 81 (1), 67–78.
Fitzgerald, P.G., Baldwin, S.L., Webb, L.E., O'Sullivan, P.B., 2006. Interpretation of (U–Th)/He single grain ages from slowly cooled crustal terranes: a case study from the Transantarctic Mountains of southern Victoria Land. Chem. Geol. 225 (1), 91–120.
Fleming, T.H., Heimann, A., Foland, K.A., Elliot, D.H., 1997. $^{40}Ar/^{39}Ar$ geochronology of Ferrar Dolerite sills from the Transantarctic Mountains, Antarctica: implications for the age and origin of the Ferrar magmatic province. GSA Bull. 109 (5), 533–546.
Foley, D.J., Stump, E., Van Soest, M., Whipple, K.X., Hodges, K.V., 2013. Differential Movement across Byrd Glacier, Antarctica, as indicated by Apatite (U–Th)/He thermochronology and geomorphological analysis. Geol. Soc. Lond. Spec. Publ. 381 (1), 7–43.
Fretwell, P., Pritchard, H.D., Vaughan, D.G., Bamr, J.L., Barrand, N.E., Bell, R., Bianchi, C., Bingham, R.G., Blankenship, D.D., Casassa, G., Catania, G., et al., 2013. Bedmap2: improved ice bed, surface and thickness datasets for Antarctica. Cryosphere 7 (1).
Galbraith, R., 1981. On statistical models for fission track counts. Math. Geol. 13, 471–478. https://doi.org/10.1007/BF01034498.
Gallagher, K., 1995. Evolving temperature histories from apatite fission-track data. Earth Planet. Sci. Lett. 136 (3), 421–435.
Gallagher, K., 2012. Transdimensional inverse thermal history modeling for quantitative thermochronology. J. Geophys. Res. Solid Earth 117 (B2).
Gallagher, K., Brown, R., 1997. The onshore record of passive margin evolution. J. Geol. Soc. 154 (3), 451–457.
Gleadow, A.J.W., Duddy, I.R., 1981. A natural long term annealing experiment for apatite. Nucl. Tracks Radiat. Meas. 5, 169–174.
Goodge, J.W., Fanning, C.M., Norman, M.D., Bennett, V.C., 2012. Temporal, isotopic and spatial relations of early Paleozoic Gondwana-margin arc magmatism, central Transantarctic Mountains, Antarctica. J. Petrol. 53 (10), 2027–2065.
Granot, R., Cande, S.C., Stock, J.M., Damaske, D., 2013. Revised Eocene–Oligocene kinematics for the West Antarctic rift system. Geophys. Res. Lett. 40, 279–284. https://doi.org/10.1029/2012GL054181.
Green, P.F., Duddy, I.R., 1989. Some comments on paleotemperature estimation from apatite fission tracks analysis. J. Pet. Geol. 12, 111–114. https://doi.org/10.1111/j.1747-5457.1989.tb00224.x.
Green, P.F., Duddy, I.R., Gleadow, A.J.W., Tingate, P.R., Laslett, G.M., 1986. Thermal annealing of fission tracks in apatite: 1. A qualitative description. Chem. Geol. 59, 237–253. https://doi.org/10.1016/0009-2541(86)90048-3.
Gunn, B.M., Warren, G., 1962. Geology of Victoria Land between the Mawson and Mulock Glaciers. N. Z. Geol. Surv. Bull. 71, 1–157.
Hamilton, R., Sorlien, C.C., Luyendyk, P., Bartek, L.R., 2001. Cenozoic tectonics of the Cape Roberts rift basin and Transantarctic Mountains front, southwestern Ross Sea, Antarctica. Tectonics 20, 325–342.
Harwood, D.M., Webb, P.N., 1998. Glacial transport of diatoms in the Antarctic Sirius Group: Pliocene refrigerator. GSA Today 8, 1–8.
Jones, S., 1997. Late Quaternary faulting and neotectonics, south Victoria Land, Antarctica. J. Geol. Soc. 154, 645–652. https://doi.org/10.1144/gsjgs.154.4.0645.
Karner, G.D., Studinger, M., Bell, R.E., 2005. Gravity anomalies of sedimentary basins and their mechanical implications: Application to the Ross Sea basins, West Antarctica. Earth Planet. Sci. Lett. 235 (3-4), 577–596.
Katz, H.R., 1982. Post-Beacon tectonics in the region of Amundsen and Scott Glaciers, Queen Maud Range, Transantarctic Mountains. Antarct. Geosci. 827–834.
Ketcham, R.A., 2005. Forward and inverse modeling of low-temperature thermochronometry data. Rev. Mineral. Geochem. 58 (1), 275–314.
Ketcham, R.A., Donelick, R.A., Donelick, M.B., 2000. AFTSolve: A program for multi-kinetic modeling of apatite fission-track data. Geol. Mater. Res. 2 (1), 1–32.
Kyle, P.R., Muncy, H.L., 1989. Geology and geochronology of McMurdo Volcanic Group rocks in the vicinity of Lake Morning, McMurdo Sound, Antarctica. Antarct. Sci. 1, 345–350.
LeMasurier, W.E., Thomson, J.W., 1990. Volcanoes of the Antarctic plate and southern oceans. Am. Geophys. Union 48.
Levy, R.H., Harwood, D.M., 2000. Sedimentary lithofacies and depositional environments of the McMurdo Sound erratics. In: Stilwell, J.D., Feldmann, R.M. (Eds.), Paleobiology and Paleoenvironments of Eocene Fossiliferous Erratics, McMurdo Sound, East Antarctica. American Geophysical Union, Antarctic Research Series, vol. 76. pp. 39–61.
Lisker, F., 2002. Review of fission track studies in northern Victoria Land, Antarctica-passive margin evolution versus uplift of the Transantarctic Mountains. Tectonophysics 349, 57–73.
Lisker, F., Läufer, A.L., 2013. The Mesozoic Victoria Basin: Vanished link between Antarctica and Australia. Geology 41 (10), 1043–1046.
Liu, H., Jezek, K., Li, B., Zhao, Z., 2001. Radarsat Antarctic Mapping Project Digital Elevation Model, Version 2. NASA National Snow and Ice Data Center Distributed Active Archive Center, Boulder, Colorado USA.
Martin, A.P., Cooper, A.F., 2010. Post 3.9 Ma fault activity within the West Antarctic rift system: onshore evidence from Gandalf Ridge, Mount Morning eruptive centre, southern Victoria Land, Antarctica. Antarct. Sci. 22, 513521. https://doi.org/10.1017/S095410201000026X.
Martin, A.P., Cooper, A.F., Dunlap, W.J., 2010. Geochronology of Mount Morning, Antarctica: two-phase evolution of a long-lived trachyte-basanite-phonolite eruptive center. Bull. Volcanol. 72, 357–371.
Mazzarini, F., Della Vedova, B., Salvini, F., 1997. Crustal segmentation of the Transantarctic Mountains rift shoulder along the David Glacier lineament, Victoria Land, Antarctica. In: Ricci, C.A. (Ed.), The Antarctic Region: Geol. Evolution and Processes. Terra Antartica Publication, Siena, pp. 565–569.
Miller, S.R., Fitzgerald, P.G., Baldwin, S.L., 2010. Cenozoic range-front faulting and development of the Transantarctic Mountains near Cape Surprise, Antarctica: Thermochronologic and geomorphologic constraints. Tectonics 29 (1).
Montgomery, D.R., Balco, G., Willett, S.D., 2001. Climate, tectonics, and the morphology of the Andes. Geology 29 (7), 579–582.
Olivetti, V., Balestrieri, M.L., Rossetti, F., Talarico, F.M., 2013. Tectonic and climatic signals from apatite detrital fission track analysis of the Cape Roberts Project core records, South Victoria Land, Antarctica. Tectonophysics 594, 80–90.
Olivetti, V., Balestrieri, M.L., Rossetti, F., Thomson, S.N., Talarico, F.M., Zattin, M., 2015. Evidence of a full West Antarctic Ice Sheet back to the early Oligocene: insight from double dating of detrital apatites in Ross Sea sediments. Terra Nova 27 (3), 238–246.
Paulsen, T.S., Wilson, T.J., 2009. Structure and age of volcanic fissures on Mount Morning: a new constraint on Neogene to contemporary stress in the West Antarctic Rift, southern Victoria Land, Antarctica. GSA Bull. 121 (7/8), 1071–1088. https://doi.org/10.1130/B26333.1.
Petit, J.P., 1987. Criteria for the sense of movement on fault surfaces in brittle rocks. J. Struct. Geol. 9, 597–608.
Pocknall, D.T., Chinn, T.J., Sykes, R., Skinner, D.N.B. 1994. Geology of the Convoy Range area, southern Victoria Land, Antarctica. Scale 1:50.000 Institute of Geol. and Nuclear Sci.
Prenzel, J., Lisker, F., Balestrieri, M.L., Läufer, A., Spiegel, C., 2013. The Eisenhower Range, Transantarctic Mountains: evaluation of qualitative interpretation concepts of thermochronological data. Chem. Geol. 352, 176–187.
Prenzel, J., Lisker, F., Monsees, N., Balestrieri, M.L., Läufer, A., Spiegel, C., 2018. Development and inversion of the Mesozoic Victoria Basin in the Terra Nova Bay (Transantarctic Mountains) derived from thermochronological data. Gondwana Res. 53, 110–128.
Rocchi, S., Armenti, P., D'Orazio, M., Tonarini, S., Wijbrans, J., Di Vincenzo, G., 2002. Cenozoic magmatism in the western Ross Embayment: role of mantle plume vs. plate dynamics in the development of the West Antarctic Rift System. J. Geophys. Res. 107 (B9), 2195. https://doi.org/10.1029/2001JB000515.
Rocchi, S., Storti, F., Di Vincenzo, G., Rossetti, F., 2003. Intraplate strike-slip tectonics as an alternative to mantle plume activity for the Cenozoic Rift Magmatismin the Ross Sea Region, Antarctica. In: Storti, F., Holdsworth, R.E., Salvini, F. (Eds.), Intraplate Strike- Slip Deformation Belts. Geological Society of London Special Publication. vol. 210. pp. 145–158.
Rossetti, F., Lisker, F., Storti, F., Läufer, A., 2003. Tectonic and denudational history of the Rennick Graben (North Victoria Land): Implications for the evolution of rifting between East and West Antarctica. Tectonics 22 (2), 1016. https://doi.org/10.1029/2002TC001416.
Rossetti, F., Storti, F., Busetti, M., Lisker, F., Di Vincenzo, G., Läufer, A., Rocchi, S., Salvini, F., 2006. Eocene initiation of Ross Sea dextral faulting and implications for East Antarctic neotectonics. J. Geol. Soc. 163, 119–126.
Salvini, F., Storti, F., 1999. Cenozoic tectonic lineaments of the Terra Nova Bay region, Ross Embayment, Antarctica. Glob. Planet. Sci. 23, 129–144.
Salvini, F., Brancolini, G., Busetti, M., Storti, F., Mazzarini, F., Coren, F., 1997. Cenozoic geodynamics of the Ross Sea region, Antarctica: Crustal extension, intraplate strike-slip faulting, and tectonic inheritance. J. Geophys. Res. Solid Earth 102 (B11), 24669–24696.
Steinberger, B., Sutherland, R., O'Connell, J., 2004. Prediction of Emperor-Hawaii seamount locations from a revised model of global plate motion and mantle flow. Nature 430, 167–173. https://doi.org/10.1038/nature02660.

Stern, T., Ten Brink, U., 1989. Flexural uplift of the Transantarctic Mountains. J. Geophys. Res. 94, 10315–10330.
Stern, T.A., Baxter, A.K., Barrett, P.J., 2005. Isostatic rebound due to glacial erosion within the Transantarctic Mountains. Geology 33 (3), 221–224.
Storti, F., Rossetti, F., Salvini, F., 2001. Structural architecture and displacement accommodation mechanisms at the termination of the Priestley Fault, northern Victoria Land, Antarctica. Tectonophysics 341, 141–161.
Storti, F., Salvini, F., Rossetti, F. Phipps, Morgan, J., 2007. Intraplate termination of transform faulting within the Antarctic continent. Earth Planet. Sci. Lett. 260, 115–126.
Storti, F., Balestrieri, M.L., Balsamo, F., Rossetti, F., 2008. Structural and thermochronological constraints to the evolution of the West Antarctic Rift System in central Victoria Land. Tectonics 27 (4).
Stump, E., 1992. The Ross Orogen of the Transantarctic Mountains in the light of the Laurentia-Gondwana split. GSA Today 2, 25–28.
Stump, E., Fitzgerald, P., 1992. Episodic uplift of the Transantarctic Mountains. Geology 20, 161–164.
Sugden, D., Denton, G., 2004. Cenozoic landscape evolution of the Convoy Range to Mackay Glacier area, Transantarctic Mountains: onshore to offshore synthesis. GSA Bull. 116 (7-8), 840–857.
Sugden, D.E., Denton, G.H., Marchant, D.R., 1995. Landscape evolution of the dry valleys, Transantarctic Mountains; tectonic implications. J. Geophys. Res. 100, 9949–9967.
Summerfield, M.A., 1991. Global Geomorphology. Prentice-Hall, New York.
Talarico, F.M., Sandroni, S., 2011. Early Miocene basement clasts in ANDRILL AND-2A core and their implications for paleoenvironmental changes in the McMurdo Sound region (western Ross Sea, Antarctica). Glob. Planet. Chang. 78, 23–35.
Talarico, F.M., McKay, R.M., Powell, R.D., Sandroni, S., Naish, T.R., 2012. Provenance signatures of the Antarctic Ice Sheets in the Ross Embayment during the Late Miocene to Early Pliocene: the ANDRILL AND-1B core record. Glob. Planet. Chang. 69, 103–123.
Tessensohn, F., Wörner, G., 1991. The Ross Sea rift system, Antarctica: structure, evolution and analogues. In: Thomson, M.R.A., Crame, J.A., Thomson, J.W. (Eds.), Geol. Evolution of Antarctica. Cambridge University Press, New York, pp. 273–277.
Turnbull, I.M., Allibone, A.H., Forsyth, P.J., Heron, D.W., 1994. Geology of the Bull Pass-St. Johns Range area, south Victoria Land, Antarctica. Geol. Map 14.
van der Beek, P., Cloetingh, S., Andriessen, P., 1994. Mechanisms of extensional basin formation and vertical motions at rift flanks: constraints from tectonic modelling and fission-track thermochronology. Earth Planet. Sci. Lett. 121 (3), 417–433.
Van der Wateren, F.M., Dunai, T.J., Van Balen, R.T., Klas, W., Verbers, A.L., Passchier, S., Herpers, U., 1999. Contrasting Neogene denudation histories of different structural regions in the Transantarctic Mountains rift flank constrained by cosmogenic isotope measurements. Glob. Planet. Chang. 23 (1), 145–172.
Vignaroli, G., Balsamo, F., Giordano, G., Rossetti, F., Storti, F., 2015. Miocene-to-Quaternary oblique rifting signature in the Western Ross Sea from fault patterns in the McMurdo Volcanic Group, north Victoria Land, Antarctica. Tectonophysics 656, 74–90.
Wannamaker, P., Hill, G., Stodt, J., Maris, V., Ogawa, Y., Selway, K., Boren, G., Bertrand, E., Uhlmann, D., Ayling, B., Green, A.M., 2017. Uplift of the central Transantarctic mountains. Nat. Commun. 17 (8(1)), 1588.
Wilson, T.J., 1995. Cenozoic transtension along the Transantarctic Mountains-West Antarctic rift boundary, Southern Victoria Land, Antarctica. Tectonics 14, 531–545.
Wilson, T.J., 1999. Cenozoic structural segmentation of the Transantarctic Mountains rift flank in Southern Victoria Land. Glob. Planet. Chang. 23, 105–127.
Wilson, T.J., Braddock, P., Janosy, R.J., Elliot, R.J., 1993. Fault kinematic studies in the Transantarctic Mountains, southern Victoria Land. Antarct. J. U. S. 26–29 (1993 Review Issue).
Wörner, G., 1999. Lithospheric dynamics and mantle sources of alkaline magmatism of the Cenozoic West Antarctic rift system. Glob. Planet. Sci. 23, 61–77.
Zachos, J., Pagani, M., Sloan, L., Thomas, E., Billups, K., 2001. Trends, rhythms, and aberrations in global climate 65 Ma to present. Science 292 (5517), 686–693.
Zattin, M., Talarico, F.M., Sandroni, S., 2010. Integrated provenance and detrital thermochronology studies in the ANDRILL AND-2A drill core: Late Oligocene–Early Miocene exhumation of the Transantarctic Mountains (Southern Victoria Land, Antarctica). Terra Nova 22, 361–368.
Zattin, M., Andreucci, B., Thomson, S.N., Reiners, P.W., Talarico, F.M., 2012. New constraints on the provenance of the ANDRILL AND-2A succession (western Ross Sea, Antarctica) from apatite triple dating. Geochem. Geophys. Geosyst. 13 (10).
Zattin, M., Pace, D., Andreucci, B., Rossetti, F., Talarico, F.M., 2014. Cenozoic erosion of the Transantarctic Mountains: a source-to-sink thermochronological study. Tectonophysics 630, 158–165.